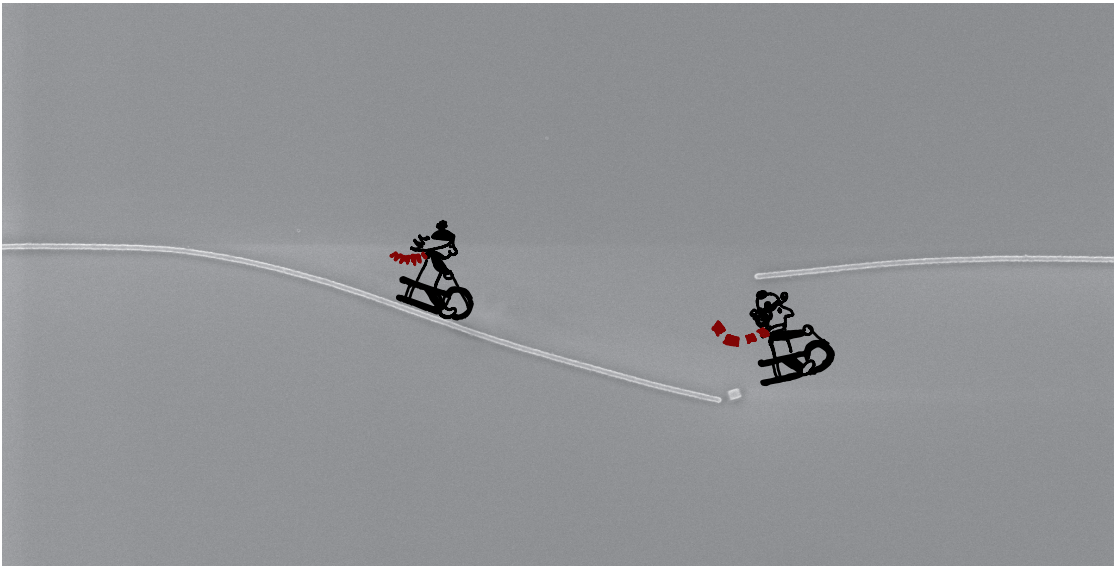




Doctoral Thesis in Physics

Integrated Photonics for Quantum Optics

SAMUEL GYGER



Integrated Photonics for Quantum Optics

SAMUEL GYGER

Academic Dissertation which, with due permission of the KTH Royal Institute of Technology, is submitted for public defence for the Degree of Doctor of Philosophy on Friday, the 10th of June 2022, at 15:00 in Brinellvägen 26, Stockholm.

Doctoral Thesis in Physics
KTH Royal Institute of Technology
Stockholm, Sweden 2022

© Samuel Gyger

Cover page image: Two doctoral students sledding on a snapped superconducting nano wire

ISBN 978-91-8040-226-2

TRITA-SCI-FOU 2022:17

Printed by: Universitetsservice US-AB, Sweden 2022

Integrated Photonics for Quantum Optics

Samuel Gyger

Albanova University Center, Departement of Applied Physics, KTH Royal Institute of Technology, SE – 106 91 Stockholm, Sweden

Abstract

Quantum physics allows us a vision of Nature’s forces that bind the world, all its seeds and sources. After decades of primarily scientific research, we’ve arrived at a stage in time where quantum technology can be applied to practical problems and add value outside the field. Four pillars of quantum technologies are commonly identified: quantum computing, quantum simulation, quantum communication, and quantum sensing. For example, quantum computers will allow us to model quantum systems beyond our current capabilities, and quantum communication allows us to protect information unconditionally based on physics. Quantum sensing will enable us to measure our reality beyond classical limits.

Within all of these areas, optical photons play a unique role. In quantum computer implementations (e.g. photonic, trapped ion, or superconducting) photons can serve as a computational resource, for system read-out, or for linking distant hardware nodes. Quantum communication can only be realized via photons, utilizing the low-loss propagation of photons in optical fibers, on photonic devices as well as in free space. In quantum sensing and metrology, squeezed light can be used to go beyond the current limits of sensing methods. Therefore, the quantum technology field crucially relies on precise and efficient methods to generate, steer, manipulate and detect photons.

This dissertation discusses work in integrated photonic circuits, self-assembled semiconductor quantum dot devices, and superconducting nanowire single-photon detectors.

We integrate multiple materials on a silicon nitride platform, including Cu_2O as a platform for solid-state Rydberg physics, WS_2 to improve non-linear light-generation within Si_3N_4 , and hBN as an excellent single-photon emitter. We demonstrate optically active quantum dots as single-photon emitters in the telecom C-band and their compatibility with commercial telecom equipment. We strain-control the fine-structure splitting of these devices, which is required for future quantum interference-based protocols.

Finally, we study superconducting nanowire single-photon detectors (SNSPD) and combine them with photonic micro-electromechanical systems (MEMS), establishing a cryo-compatible, reconfigurable photonic platform.

Key words: integrated photonics, single-photons, single-photon sources, single-photon detectors, SNSPD

Integrerad Fotonik för Kvantoptik

Samuel Gyger

Institutionen för Tillämpad fysik, Kungliga Tekniska högskolan,
SE-106 91 Stockholm, Sverige

Sammanfattning

Kvantfysiken ger oss en möjlighet att skåda naturens krafter som binder världen, alla dess frön och källor. Efter decennier av främst vetenskaplig forskning har vi nått det stadiet i tiden där kvantteknologi kan tillämpas på praktiska problem och tillföra värde utanför akademien. Vanligtvis identifieras fyra pelare av kvantteknologier: kvantberäkning, kvantsimulering, kvantkommunikation och kvantsensorer. Till exempel kommer kvantdatorer att tillåta oss att modellera kvantsystem utöver våra nuvarande möjligheter, och kvantkommunikation tillåter oss att skydda information villkorslöst baserat på fysikens lagar samtidigt som kvantavkänning kommer att göra det möjligt för oss att mäta vår verklighet bortom klassiska gränser.

Inom alla dessa områden spelar optiska fotoner en unik roll. I kvantdatorimplementationer (t.ex. fotoniska, fångade joner eller supraledande) kan fotoner fungera som en beräkningsresurs, för systemavläsning eller för att länka avlägsna hårdvaru-noder. Kvantkommunikation kan endast förverkligas via fotoner, på grund av den låga förlusten av fotoner i optiska fibrer, på fotoniska enheter såväl som i fri luft. Inom kvantavkänning och metrologi kan klämt ljus användas för att överskrida de nuvarande gränserna för avkänningsmetoder. Därför förlitar sig kvantteknikområdet på exakta och effektiva metoder för att generera, styra, manipulera och detektera fotoner.

Den här avhandlingen diskuterar arbete i integrerade fotoniska kretsar, självmonterade halvledarkvantpricksenheter och supraledande nanotrådsdetektorer för enstaka fotoner.

Vi integrerar flera material på en kiselnitridplattform, inklusive Cu_2O som en plattform för rydbergs fysik i fast tillstånd, WS_2 för att förbättra icke-linjär ljusgenerering inom Si_3N_4 och hBN som utmärkt singelfoton-sändare. Vi demonstrerar optiskt aktiva kvantprickar som enstaka foton sändare i telekom C-bandet och deras kompatibilitet med kommersiell telekomutrustning. Vi kontrollerar finstruktursdelningen av dessa enheter med hjälp av töjning, vilket krävs för framtida kvantinterferensbaserade protokoll.

Slutligen studerar vi supraledande nanotrådsdetektorer för enstaka fotoner och kombinerar dem med fotoniska mikroelektromekaniska system, vilket skapar en kryokompatibel, konfigurerbar fotonisk plattform.

Nyckelord: integrerad fotonik, enstaka fotoner, enstaka fotonkällor, kvantprickar, enstaka fotondetektorer, SNSPDs

Preface

This thesis describes the work done by Samuel Gyger (SG) and the team working within Quantum Nano Photonics (QNP) at the KTH Royal Institute of Technology with the help of many collaborators. We use multiple material systems to generate, manipulate and detect single photons. We design and demonstrate various integrated photonic elements including Cu_2O , 2D materials, and SNSPDs based on NbTiN

My work was funded by the Swedish Research Council under Grant Agreement No. 2016-06122 (Optical Quantum Sensing).

Paper 1. S. GYGER, J. ZICHI, L. SCHWEICKERT, A. W. ELSHAARI, S. STEINHAEUER, S. F. COVRE DA SILVA, A. RASTELLI, V. ZWILLER, K. D. JÖNS AND C. ERRANDO-HERRANZ, 2021. *Reconfigurable Photonics with On-Chip Single-Photon Detectors*. Nat. Commun **12** (1), 1408.

Paper 2. S. STEINHAEUER, M. A. M. VERSTEEGH, S. GYGER, A. W. ELSHAARI, B. KUNERT, A. MYSYROWICZ, AND V. ZWILLER, 2020. *Rydberg excitons in Cu_2O microcrystals grown on a silicon platform*. Commun Mater **1** (1), 1-7.

Paper 3. Y. WANG,[†] V. PELGRIN,[†] S. GYGER, G. M. UDDIN, X. BAI, C. LAFFORGUE, L. VIVIEN, K. D. JÖNS, E. CASSAN, AND Z. SUN, 2021. *Enhancing Si_3N_4 Waveguide Nonlinearity with Heterogeneous Integration of Few-Layer WS_2* . ACS Photonics **8** (9), 2713-2721.

Paper 4. A. W. ELSHAARI,[†] A. SKALLI,[†] S. GYGER, M. NURIZZO, L. SCHWEICKERT, I. E. ZADEH, M. SVEDENDAHL, S. STEINHAEUER, AND V. ZWILLER, 2021. *Deterministic Integration of HBN Emitter in Silicon Nitride Photonic Waveguide*. Adv. Quantum Technol. **4** (6), 2100032.

Paper 5. J. KLEIN,[†] L. SIGL,[†] S. GYGER, K. BARTHELMI, M. FLORIAN, S. REY, T. TANIGUCHI, K. WATANABE, F. JAHNKE, C. KASTL, V. ZWILLER, K. D. JÖNS, K. MÜLLER, U. WURSTBAUER, J. J. FINLEY, AND A. W. HOLLEITNER, 2021. *Engineering the Luminescence and Generation of Individual Defect Emitters in Atomically Thin MoS_2* . ACS Photonics **8** (2), 669-677.

Paper 6. S. GYGER,[†] K. D. ZEUNER,[†] K. D. JÖNS, A. W. ELSHAARI, M. PAUL, S. POPOV, C. REUTERSKIÖLD HEDLUND, M. HAMMAR, O. OSZOLINS, AND V. ZWILLER, 2019. *Reconfigurable frequency coding of triggered single photons in the telecom C-band*. Opt. Express **27**, 14400-14406.

Paper 7. T. LETTNER, S. GYGER, K. D. ZEUNER, L. SCHWEICKERT, S. STEINHAEUER, C. REUTERSKIÖLD HEDLUND, S. STROJ, A. RASTELLI,

M. HAMMAR, R. TROTTA, K. D. JÖNS, AND V. ZWILLER, 2021. *Strain-Controlled Quantum Dot Fine Structure for Entangled Photon Generation at 1550 nm*. Nano Lett. **21** (24), 10501–10506.

Paper 8. S. STEINHAEUER, L. YANG, S. GYGER, T. LETTNER, C. ERRANDO-HERRANZ, K. D. JÖNS, M. A. BAGHBAN, K. GALLO, J. ZICHI, AND V. ZWILLER, 2020. *NbTiN Thin Films for Superconducting Photon Detectors on Photonic and Two-Dimensional Materials*. Appl. Phys. Lett. **116** (17), 171101.

Paper 9. S. STEINHAEUER, S. GYGER, AND V. ZWILLER, 2021. *Progress on large-scale superconducting nanowire single-photon detectors*. Appl. Phys. Lett. **118**, 100501.

June 2022, Stockholm
Samuel Gyger

†: Authors contributed equally.

Author contributions

The main advisor for the thesis is Prof. Dr. Val Zwiller (VZ).

I was co-supervised by Dr. Stephan Steinhauer (SS), Prof. Dr. Ali W. Elshaari (AE) and Dr. Marijn Versteegh (MV).

I outlined my contributions (SG) in the publications below.

Paper 1. Fabrication of devices by C. Errando-Herranz (CEH). Development of SNSPD fabrication process on SiN by SG. Building of measurement setup by SG. Measurements together with CEH. Development of demonstrator experiments with input from CEH, Klaus D. Jöns (KJ) and VZ. Evaluation of the measurement data by SG and CEH. Preparation of the manuscript with CEH and input from the other authors.

Paper 2. Fabrication of waveguide devices by SG and SS. Development of SiN fabrication process by AE. Room temperature waveguide measurement built by AE and SG. WG measurements by SG, AE, and SS. Manuscript preparation by SS with input from the other authors.

Paper 3. Fabrication of bare SiN waveguide devices by SG. Input on manuscript preparation from SG. Manuscript preparation by Yuchen Wang with input from the other authors.

Paper 4. Cryogenic measurement setup built by SG. Measurements at cryogenic temperatures by SG and Anas Skalli. Input on manuscript preparation by SG.

Paper 5. Measurement of single-photon characteristics (g^2) by SG und KJ. Data evaluation of time-correlation data by SG. Input on manuscript preparation by SG.

Paper 6. Measurement of QD properties, time-correlation, and electro-optical modulation together with Katharina D. Zeuner (KDZ). Preparation of the manuscript with KDZ.

Paper 7. Correlation and Entanglement measurements together with Thomas Lettner (TL). Input on data preparation by SG. Input on manuscript preparation by SG.

Paper 8. Film development and deposition by Julien Zichi (JZ). Fabrication of SNSPDs on films by SG. Measurement of SNSPDs together with SS. Input on data evaluation by SG. Manuscript preparation and project management by SS.

Paper 9. Collection of data for comparison of the field by SG. Input on manuscript preparation by SG. Concept and manuscript preparation by SS with input from the other authors.

Other publications

The following papers, although related, are not included in this thesis.

A. W. ELSHAARI,[†] E. BÜYÜKÖZER,[†] I. E. ZADEH, T. LETTNER, P. ZHAO, E. SCHÖLL, S. GYGER, M. E. REIMER, D. DALACU, P. J. POOLE, K. D. JÖNS, AND V. ZWILLER, 2018. *Strain-Tunable Quantum Integrated Photonics*. Nano Lett. **18** (12), 7969–7976.

K. BARTHELMI, J. KLEIN, A. HÖTGER, L. SIGL, F. SIGGER, E. MITTERREITER, S. REY, S. GYGER, M. LORKE, M. FLORIAN, F. JAHNKE, T. TANIGUCHI, K. WATANABE, V. ZWILLER, K. D. JÖNS, U. WURSTBAUER, C. KASTL, A. WEBER-BARGIONI, J. J. FINLEY, K. MÜLLER, AND A. W. HOLLEITNER, 2018. *Atomistic Defects as Single-Photon Emitters in Atomically Thin MoS₂*. Appl. Phys. Lett. **117** (7), 070501.

T. LETTNER, K. D. ZEUNER, E. SCHÖLL, H. HUANG, S. SCHARMER, S. F. C. DA SILVA, S. GYGER, L. SCHWEICKERT, A. RASTELLI, K. D. JÖNS, AND V. ZWILLER, 2020. *GaAs Quantum Dot in a Parabolic Microcavity Tuned to ⁸⁷Rb D₁*. ACS Photonics **7** (1), 29–35.

C. ERRANDO-HERRANZ,[†] E. SCHÖLL,[†] R. PICARD, M. LAINI, S. GYGER, A. W. ELSHAARI, A. BRANNY, U. WENNBURG, S. BARBAT, T. RENAUD, M. SARTISON, M. BROTONS-GISBERT, C. BONATO, B. D. GERARDOT, V. ZWILLER, AND K. D. JÖNS, 2021. *Resonance Fluorescence from Waveguide-Coupled, Strain-Localized, Two-Dimensional Quantum Emitters*. ACS Photonics **8** (4), 1069–1076.

I. E. ZADEH, J. CHANG, J. W. N. LOS, S. GYGER, A. W. ELSHAARI, S. STEINHAEUER, S. N. DORENBOS, AND V. ZWILLER, 2021. *Superconducting Nanowire Single-Photon Detectors: A Perspective on Evolution, State-of-the-Art, Future Developments, and Applications*. Appl. Phys. Lett. **118** (19), 190502.

A. HÖTGER, J. KLEIN, K. BARTHELMI, L. SIGL, F. SIGGER, W. MÄNNER, S. GYGER, M. FLORIAN, M. LORKE, F. JAHNKE, T. TANIGUCHI, K. WATANABE, K. D. JÖNS, U. WURSTBAUER, C. KASTL, K. MÜLLER, J. J. FINLEY, AND A. W. HOLLEITNER, 2018. *Gate-Switchable Arrays of Quantum Light Emitters in Contacted Monolayer MoS₂ van Der Waals Heterodevices*. Nano Lett. **21** (2), 1040–1046.

Z. LIN,[†] L. SCHWEICKERT,[†] S. GYGER, K. D. JÖNS, AND V. ZWILLER, 2020. *Efficient and Versatile Toolbox for Analysis of Time-Tagged Measurements*. J. Inst. **16** (08), T08016.

K. D. ZEUNER, K. D. JÖNS, L. SCHWEICKERT, C. R. HEDLUND, C. N. LOBATO, T. LETTNER, K. WANG, S. GYGER, E. SCHÖLL, S. STEINHAEUER, M. HAMMAR, AND V. ZWILLER, 2021. *On-Demand Generation of Entangled Photon Pairs in the Telecom C-Band with InAs Quantum Dots*. ACS Photonics **8** (8), 2337–2344.

- M. SIDOROVA, A. D. SEMENOV, H.-W. HÜBERS, S. GYGER, S. STEINHAUER, X. ZHANG, AND A. SCHILLING, 2021. *Magnetoconductance and Photoresponse Properties of Disordered NbTiN Films*. Phys. Rev. B **104** (18), 184514.
- M. A. M. VERSTEEGH, S. STEINHAUER, J. BAJO, T. LETTNER, A. SORO, A. ROMANOVA, S. GYGER, L. SCHWEICKERT, A. MYSYROWICZ, AND V. ZWILLER, 2021. *Giant Rydberg Excitons in Cu₂O Probed by Photoluminescence Excitation Spectroscopy*. Phys. Rev. B **104** (24), 245206.
- N. HU, Y. MENG, K. ZOU, Y. FENG, Z. HAO, S. STEINHAUER, S. GYGER, V. ZWILLER, X. HU, 2022. *Full-Stokes polarimetric measurements and imaging using a fractal superconducting nanowire single-photon detector*. Optica **9** (4), 346–351.

Contents

Abstract	iii
Sammanfattning	iv
Preface	v
List of Abbreviations	xiv

Part I - Overview and Summary

Chapter 1. Introduction	1
1.1. Quantum Optics - Beyond Classical Light	2
1.2. Integrated Optics - Miniaturize and Scale	2
1.3. Integrated Photonics for Quantum Optics	3
1.4. Research Presented in the Thesis	3
1.5. Structure of the Thesis	5
Chapter 2. Guiding Light on Chip	
Integrated Photonics	6
2.1. Simulation of Photonic Circuits	8
2.2. Material Stacks for Photonic Circuits	9
2.3. Building Blocks of Photonic Circuits	10
2.4. Reconfigurability of Photonic Circuits	11
2.5. Hybrid Integration on Photonic Circuits	13
Chapter 3. Creating Single Photons	
Quantum Optics	17
3.1. Single Photon: What Does It Mean?	17
3.2. Single Photons: What Do We Want?	19
3.3. Photoluminescence Setup. Extracting Single Photons	20
3.4. HBT-Measurement. Proofing Single Photon Character	22

3.5.	Crystal Defects: Single Photon Sources	23
3.6.	2D Materials: "Single-Layer" Quantum Dots	24
3.7.	Quantum Dots: Large Scale, Artificial Atoms	25
Chapter 4.	Manipulating Single Photons	
	Quantum Optics	27
4.1.	Electro-optic Modulation for Single Photons	27
4.2.	Fine-structure Tuning using Strain	30
Chapter 5.	Detecting Single Photons	
	Quantum Optics	33
5.1.	Requirements for Single-Photon Detection	33
5.2.	Superconducting Nanowire Single Photon Detectors (SNSPD)	34
5.3.	Measuring Properties of SNSPDs	37
5.4.	Multiplexing and Scale-Up of SNSPDs	40
5.5.	Waveguide-Integrated SNSPDs	42
Chapter 6.	Conclusions and Outlook	45
	Acknowledgments	49
	Bibliography	52

Part II - Papers

Summary of the Papers	71
Paper 1. Reconfigurable Photonics with On-Chip Single-Photon Detectors	75
Paper 2. Rydberg excitons in Cu ₂ O microcrystals grown on a silicon platform	85
Paper 3. Enhancing Si ₃ N ₄ Waveguide Nonlinearity with Heterogeneous Integration of Few-Layer WS ₂	95
Paper 4. Deterministic Integration of HBN Emitter in Silicon Nitride Photonic Waveguide	107
Paper 5. Engineering the Luminescence and Generation of Individual Defect Emitters in Atomically Thin MoS ₂	119
Paper 6. Reconfigurable frequency coding of triggered single photons in the telecom C-band	131
Paper 7. Strain-Controlled Quantum Dot Fine Structure for Entangled Photon Generation at 1550 nm	141
Paper 8. NbTiN Thin Films for Superconducting Photon Detectors on Photonic and 2D Materials	149
Paper 9. Progress on large-scale superconducting nanowire single-photon detectors	157

List of Abbreviations

AlGaAs	Aluminium gallium arsenide
GaAs	Gallium arsenide
GaP	Gallium phosphide
HeNe	Helium-neon laser
InAs	Indium arsenide
InGaAs	Indium gallium arsenide
InP	Indium phosphide
LiNbO₃	Lithium niobate
NbTiN	Niobium titanium nitride
Si	Silicon
SiC	Silicon carbide
SiN	Silicon nitride
SiO₂	Silicon dioxide
BOX	Buried oxide
BS	Non-polarizing beam splitter
CCD	Charge-coupled device
CW	Continuous wave
DBR	Distributed Bragg reflector
DCR	Dark count rate
EOM	Electro-optic modulator
FDTD	Finite-domain time-difference
FEM	Finite element method
FSS	Fine structure splitting
HBT	Hanbury Brown and Twiss
IC	Integrated circuit
III-V	Compound semiconductor formed from group III and V
KTH	KTH Royal Institute of Technology in Stockholm
LIDAR	Light detection and ranging
LIGO	Laser interferometer gravitational-wave observatory
MEMS	Micro-electromechanical systems
MOM	Method of moments
NEP	Noise-equivalent power
PCR	Photon count rate

PDK	Process design kit
PIC	Photonic integrated circuit
PMT	Photo-multiplier tube
QD	Quantum dot
QKD	Quantum key distribution
QNP	Quantum Nano Photonics (research group at KTH)
S(N)SPD	Superconducting (nanowire) single-photon detector
SEM	Scanning electron microscope
SFQ	Single flux quantum
SNR	Signal-to-noise ratio
SOI	Silicon on insulator
T	Trion
TS	Transmission spectrometer
X	Exciton
XX	Biexciton

Part I

Overview and Summary

Introduction

Light is the human's window into physical reality. Beyond the image generated in our eyes to navigate our daily lives, which poses additional challenges if it is missing, it enables us to examine everything from atoms to galaxies, measure distances in buildings, and analyze PCR tests.

The interest in understanding light can be traced back to the Greek traditions around 800 BC. Before the nineteenth century, people thought of light as particles because Newton (1642 to 1727), who regarded light as little corpuscles, said so. It was Thomas Young's (1773 to 1829) experiment of the double-slit in 1802 that changed the general perception and led to the acceptance of light's wave nature. It would require a second revolution in the understanding of light to reintroduce the light particle. In 1905, Albert Einstein, building on the work of his contemporaries, theorized light as energy packets[1]. The concept of the photon was resurrected.

Photonics, named after said photon, is the scientific and engineering discipline of generating, manipulating, and detecting light for practical applications.¹ In this thesis, we will look at light close to the visible spectrum from 530 nm to 1600 nm, but any electro-magnetic signal is made of photons, from the radio signal necessary for listening to the news to gamma rays emitted by radiative decay.

Following the re-discovery of photons as particles, it was first unclear how to characterize the disparity between wave and particle. Paul Dirac proposed in 1927 the use of a harmonic oscillator for each existing electro-magnetic mode[2]. This allowed us to move beyond quantizing only atoms interacting with a classical field, but quantizing atomic energy levels interacting with quantized light. When in 1963 Roy Glauber asked and answered the question, "What distinguishes light sources?", the field of quantum optics was born[3], [4]. It is now another 60 years later that the field, in the second quantum revolution[5], promises to increase measurement sensitivity, provide new computing resources, and control systems down to the single particle.

¹Optics, in my opinion and arbitrary, is the field that is doing the same for the sake of discovery.

1.1. Quantum Optics - Beyond Classical Light

The answer to the question of the difference between a torch, a laser, and a single photon source can be found in the different photon statistics (see also section 3.1). This difference was observed in the Hanbury Brown-Twiss (HBT) experiment[6] (see section 3.4), a measurement correlating photon detection times. It became clear that there are types of light that cannot be classically described. Several milestone experiments were conducted in the decades following the HBT experiments. In 1977 photon antibunching was demonstrated [7], in 1985 squeezed light was demonstrated[8] and in 1987 Hong-Ou-Mandel demonstrated photon indistinguishability[9]. While in the early years deeper understanding of physics was enabled through quantum optics, the developed techniques have recently begun to be used in practical problems or to support other scientific disciplines[10]. An example is squeezed light which can be used to sense beyond the shot-noise limit[11]. It has been used to reduce noise in the search for gravitational waves using LIGO[12]. Quantum information science is another field that is rooted within quantum optics. A paper by Richard Feynman in June 1982 proposing to simulate physics using quantum computers is widely regarded as the first proposal for quantum computing[13]. Since then, there has been a surge in interest in quantum computing, fueled by successful demonstrations of quantum advantage for tailored problems in 2019[14]. A summary of multiple platforms in quantum computing can be found in this review by Ladd et al.[15]. As the last example, quantum communication provides communication secured by the laws of physics[16], [17] and in the long term will allow to share entanglement between computing nodes[18] or build "single" telescopes spanning the world[19].

1.2. Integrated Optics - Miniaturize and Scale

The idea of guiding light on a chip is similar to how current is guided in integrated electronic circuits for analog (e.g. amplification) and digital (e.g. calculation) functions. The fact that the same material, silicon, may be utilized for both applications is an incredible coincidence. Silicon photonics became the dominant photonic platform after the discovery of the free carrier dispersion effect in 1987[20]. Since then integrated photonics has been used to build transceivers for receiving and transmitting data over an optical signal, or to split wavelengths using arrayed waveguide gratings and send signals in different optical channels coupled to multiple photodiodes. Frequency combs on chips are used to create light at many wavelengths from a single laser, and switching matrices with a port count of up to 128×128 , relevant e.g. in data-centers[21], can be built. Photonic platforms are available in multiple foundries around the world offering shared (so-called multi-project wafers) and distinct processes with an overall estimated market of around 1 billion dollars[22].

A recent review of silicon photonics is written by Siew et al.[23] and of silicon nitride photonics by Blumenthal et al.[24].

1.3. Integrated Photonics for Quantum Optics

To scale quantum technologies beyond demonstrations of principle it is unavoidable to utilize scalable fabrication technologies. With the integrated photonics market's success and size, it's an obvious path to use this resource to support quantum optics and develop quantum technologies. This combined field called integrated quantum photonics[25] combines traditional photonic elements with elements developed in bulk quantum optics experiments. One of the early integrated quantum optics experiments implemented a Quantum Key Distribution (QKD) system in 2004[26]. Since then people have demonstrated amongst others an integrated CNOT gate, Boson sampling, single photon generation on-chip, and multiple quantum algorithms[27].

The integrated platform provides several benefits such as a small footprint, high phase stability, and manufacturing scalability. One of the disadvantages is that high-performing optical components were optimized for a long time in bulk optics, and need to be redeveloped separately for every integrated platform. Still integrated quantum optics is the way to go for bringing quantum applications to market while also supporting next-generation quantum optics and physics experiments[28].

1.4. Research Presented in the Thesis

This thesis contains the fabrication and measurement of integrated photonic devices. Single photons are generated using self-assembled quantum dots as well as emission centers within hBN and MoS₂. Waveguides, based on Si₃N₄, are fabricated and single-photon detectors, based on NbTiN, are integrated and tested.

In **Paper 1** we co-integrate superconducting nanowire single photon detectors (SNSPDs) with electro-statically movable silicon nitride waveguides based on photonic micro-electromechanical systems (MEMS). We show process compatibility and demonstrate a high dynamic range power meter, feedback power control on-chip, and the static routing of single photons on-chip.

In **Paper 2** we investigate the integration of synthetic Cu₂O crystals with SiN waveguide. We demonstrate excitonic luminescence through the waveguide at room temperature.

In **Paper 3** we investigate the enhancement of the non-linearity in SiN for continuum light generation through hybrid integration of WS₂.

In **Paper 4** we investigate individual emitters created in hBN through thermal annealing and encapsulate them preselected in SiN based waveguides. We measure their single-photon emission at room temperature and ≈ 200 mK.

In **Paper 5** we investigate individual emitters created by focused helium-ion beam irradiation [29] and proof their single-photon characteristics. We show a creation probability of single emitters $> 18\%$ and investigate the influence of the order of the fabrication steps.

In **Paper 6** we use triggered single photons generated in the telecom C-band and implement a beam-splitter in frequency using a phase modulator. We then filter the sidebands and measure cross-correlation of the sidebands with a single-photon purity of $g^{(2)} = 0.16 \pm 0.06$.

In **Paper 7** we measure triggered entangled single photon generated in the telecom C-band. They exhibit a fine-structure splitting (FSS) between the entangled bases, which is detrimental to their application. We reduce the FSS using strain applied by a piezo with six actuators. We measure entanglement fidelity for multiple FSS settings and detector time resolutions.

In **Paper 8** we evaluate the performance of a superconducting film developed within our group [30] on multiple photonic platforms. We show the properties and performance of SNSPD are weakly influenced. This highlights the stable properties of NbTiN for different substrates. Optimizing the film for each different substrate becomes less important.

In **Paper 9** we summarize the state of the art for increasing the pixel size and the pixel number of SNSPDs device.

1.5. Structure of the Thesis

This thesis contains two parts.

Part I anchors the research work within the field. It presents a short and selective overview of integrated photonics, single photon emitters, and single photon detection. The goal is for the reader to understand the place of the thesis work within the field. The thesis does not contain a lot of unpublished knowledge, so a searching reader should probably look elsewhere. Wherever possible, I try to highlight other useful literature to read further.

Part II summarizes and includes nine publications and is the main work forming this thesis. The results were created based on the fabrication processes and measurement tools that were developed as part of the thesis. More publications created during the time of the thesis are listed on page viii.

Chapter 1 introduces the field of quantum optics, the use of quantum states of light, and integrated photonics, a technology used for the miniaturization of light-based circuits on integrated chips. It draws attention to the solutions where the former can benefit from the latter. This then leads to the goals and structure of the thesis.

Chapter 2 covers the technology of integrated photonics. It discusses guiding light in dielectric structures as well as methods for simulating such structures before fabrication. The material platforms used within the work of this thesis are presented. Key building blocks are highlighted. Methods for reconfigurability are presented and used in **Paper 1**. To expand the functionality of the material platforms, hybrid integration methods are presented, with two examples from **Paper 2** and **Paper 3**.

Chapter 3 discusses the process of generating single photons. It introduces the figure of merits for single photons and describes the measurement tools used within this thesis. Several different sources for single photons are introduced and used in **Paper 4**, **Paper 6**, and **Paper 5**.

Chapter 4 discusses the possibilities opened by manipulating single photons. Two examples are discussed, the modulation using an electro-optic modulator in **Paper 6** and the influence on the source by tri-axial strain in **Paper 7**.

Chapter 5 discusses methods to detect single photons. It then introduces the leading technology today, Superconducting Nanowire Single Photon Detectors (SNSPD). The future of the SNSPDs in terms of scaling is discussed based on **review Paper 9**. A highly substrate-compatible superconducting film (**Paper 8**) is used to implement SNSPD on waveguides **Paper 1**.

Chapter 6 attempts to provide an outlook on what lies ahead for quantum optics utilizing integrated photonics, as well as where developments from this thesis can fit in.

Guiding Light on Chip

Integrated Photonics

Guiding light within confined structures has enabled the world to be connected using fiber-optic cables, the backbone for any internet technology. Fiber expansion has accelerated in recent decades to support average download speeds predicted to reach 250 Mbit s^{-1} megabits per second in 2024[31]. Our economy, work, leisure time, and physical well-being are all linked to services made possible by fiber deployments. The enabling principle is a refractive index difference that allows for the confinement of a light beam (called mode) in a certain area, called the core. The refractive index¹ is a measure of the speed at which light may travel through a material. For glass fibers this is a region with a higher refractive index, that is created through doping. A typical fiber (SMF-28) deployed today has a typical refractive index difference of 0.36 % [32].

The same principle can be used to confine light to planar structures on a chip to develop complex networks. Initial devices were created by doping areas within the chip, but the difference in refractive index is small (e.g. for lithium niobate a difference of $< 0.5 \%$ [33]) which leads to very leaky guiding when sharper bends are introduced. Small footprint waveguides with a bending radius of less than $100 \mu\text{m}$ can be made possible by increasing the refractive index contrast between the guiding area (core) and the surrounding material (cladding). In photonic chips, this is achieved by patterning the material forming the core into so-called waveguides. A typical stack is using silicon encapsulated in silicon dioxide with an index difference of a factor of ≈ 2.4 . This allows for the integration of much more functionality on a chip such as integrated transceivers for high-speed datacenters, small footprint Light Detection and Ranging (LIDAR) systems, or optical computing units.

Nowadays photonic integrated circuits (PIC) can be ordered similar to electronic integrated circuits (IC) without having advanced nanofabrication facilities at hand[23]. Multiple platforms are available and this fabless fabrication allows small and large companies to develop new applications with standardized processes, guaranteed yields, but also long lead times[34].

¹A large collection of refractive index data can be found on <https://refractiveindex.info/>

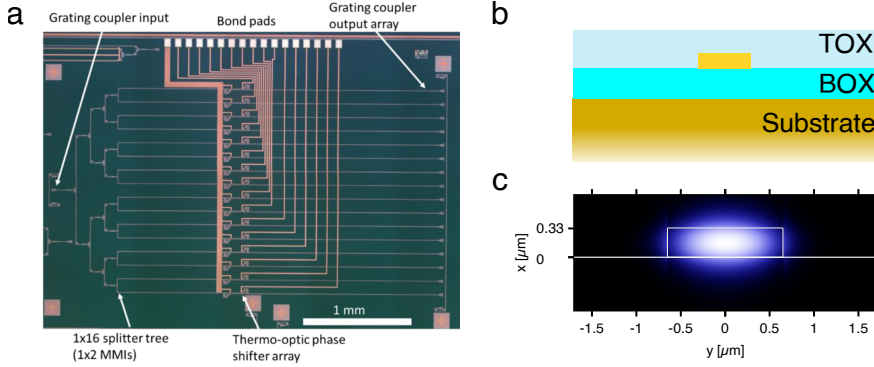


Figure 2.1: **Dielectric on Insulator: a platform for integrated photonics.** a) Integrated Photonic Chip on a silicon platform. Including beam-splitter, thermal phase shifters, and grating coupler to get light on and off the chip. b) Typical cross-section of the optical stack. A waveguide lies on top of an oxide layer (BOX) e.g. silicon dioxide supported by a substrate, typically silicon. Everything is optionally covered with another layer of oxide (here denoted TOX) c) Optical mode profile of the fundamental mode's electromagnetic field within a typical waveguide. Created using the EIMS tool[35]. Adapted with permission from [36].

An exemplary photonic chip created in IMEC, a European photonic foundry, is shown in Figure 2.1a[36]. It consists of waveguides, beamsplitters, tunable elements, and grating couplers to bring light on and off-chip. The cross-section of a typical chip is shown in Figure 2.1b. The light is guided predominantly in the core of the waveguide with typical heights between 150 nm to 400 nm. The carrier of the circuit, called substrate, is often silicon but can be other (often crystalline) material. The core is separated from the substrate by a layer of bottom cladding, often called BOX layer for buried oxide. To symmetrize the dielectric environment of the core a top cladding is introduced (here called TOX layer for top oxide). It is also required if metal layers for electrodes need to cross the waveguides. While indium phosphide (InP) and silicon as core materials are dominating today, many material platforms exist with an overview covered in Section 2.2.

The waveguide core supports modes, which are distinct configurations of light intensities. A typical optical mode profile of the electromagnetic field is shown in Figure 2.1c. While the majority of the power is contained within the waveguide's core, some field energy leaks outside. Section 2.5 discusses how this can be used to interact with surrounding materials.

Propagation losses are an important parameter for integrated photonics. They are caused by multiple sources. On the lower end, they are limited by the

internal losses of the guiding material. Outside of the operating wavelength regime, this is the dominating loss, e.g. blue light within SiN waveguides is absorbed while light at $\lambda_0 = 1550\text{ nm}$ has been demonstrated with losses below 1 dB m^{-1} [37], [38] Another source is **side-wall roughness** given by the lithography and etching processes. This is the main loss mechanism in a waveguide fabricated in our university cleanroom. Roughness between BOX and core and on the top surface of the core can lead to scattering loss into the bottom cladding or top cladding[39]. Stitching errors between different write fields of the lithography system will lead to localized loss sites. And at last, there can be mistakes in the design such as sharp bends in the waveguide, that lead to radiation losses.

The chapter will discuss methods for simulating photonic circuits, provide an overview of the material stacks used in the thesis, and introduce common building blocks for photonic circuits. Tunable circuit technologies are discussed, as well as the hybrid integration of different material systems.

2.1. Simulation of Photonic Circuits

Producing a photonic chip requires several fabrication steps in a prototyping clean-room or several weeks to months of fabrication in a commercial wafer run. Fortunately, electromagnetic waves, of which light is a type, can be extremely successfully simulated using commercial and research software. The leading methods employed in photonics today are the finite-domain time-difference method (FDTD) and the finite element method (FEM). In the microwave domain, the method of moments (MOM) is commonly used[40]. The different methods are described briefly below with the software used during the thesis in bold.

FDTD was introduced in the seventies[41], based on an algorithm of Yee[42]. The technique is a brute-force method of solving the problem in the time domain. This leads to broad-band data being available after solving the problems once. Good implementations for absorbing boundary conditions exist (PML) and material properties can be defined easily. The main drawback is the required rectangular mesh. Several software packages exist among them **Lumerical** and **MEEP**. Lumerical is commercial software, often used in photonic research. It features a GUI, scripting capabilities, and a low entry barrier. MEEP is open-source with a lot of activity in recent years. The geometry is scripted and a Python interface exists. It includes the majority of the features required for simulation, except non-uniform meshing, which is the most notable omission.

FEM can solve differential equations on non-rectangular meshes. Mechanical design and structural analysis make extensive use of the approach. It has also been used to solve partial differential equations in other disciplines. It can be used in electromagnetics to solve Maxwell's equation in both frequency and time domains, with the former being the more popular. Broadband solutions need a large amount of computing time due to the solution being in frequency space. The mesh generation procedure is time-consuming and has a large impact on

the obtained outcomes. A selection of software packages is **COMSOL**, CST Studio, JCMWave, and ANSYS HFSS.

MOM is a method to solve electromagnetic problems within the frequency domain. It is commonly used for microwave circuits and antennas, with high efficiency for highly conductive surfaces. A selection of software packages is FEKO and **Sonnet**. The latter we used during this thesis, as a planar solver for microwave engineering of PCBs and superconducting thin films.

2.2. Material Stacks for Photonic Circuits

Several material systems are currently employed to build photonic circuits. They are characterized by their different properties: transparent region, direct or indirect bandgap, non-linearities, and refractive index contrast. The dominant workhorses today in the industry are silicon photonics and indium phosphide (InP) platforms[43]. The former provides tunable circuits, low losses, and compatibility with CMOS-based electronic foundries. The disadvantage is that no direct light sources exist. InP on the other hand provides on-chip lasers and amplifiers but is typically fabricated on 3-inch wafers due to material handling challenges, which leads to a higher cost per device. As the stack is usually based on lattice-matched substrates, the refractive index contrast is limited. Next to these well-established material stacks with commercial foundries, a large collection of other materials is being pursued. One promising avenue is the study of compound semiconductors on insulators, in which a crystalline thin-film is transferred onto a lower refractive index dielectric[44]. This enables a separate optimized growth for the film layer that provides high-quality material properties.

A summary of popular photonic platforms with important properties is given in Table 2.1. It shows the type of bandgap (a direct bandgap is relevant for light sources on-chip), the highest achieved Q factor (relevant for the expected optical loss), the index contrast between silicon dioxide and the material, as well as χ_2 and n_2 for nonlinear processes of the second and third-order.

Two material stacks were used during this thesis, silicon nitride and lithium niobate.

Silicon nitride on Insulator (**SiNOI**)[56] is a photonic material that has gotten a lot of attention in the last few decades for linear[57] and non-linear [58] integrated photonics. It combines several favorable characteristics, including very low optical losses ($< 3 \text{ dB m}^{-1}$ [59]), a large enough refractive index to be used on top of SiO_2 , no two-photon absorption above 800 nm, high power tolerance, and high Kerr nonlinearity as well as wafer-scale processing[38]. Most of the results obtained during the work on this thesis are based on a silicon nitride platform. (Paper 2, Paper 1, Paper 3, Paper 4)

Lithium niobate on Insulator (**LNOI**)[60] is a thin-film platform using the well-established electro-optical material lithium niobate (LiNbO_3)[61], [62]. First demonstrated around the turn of the millenial[63], [64], within a decade propagation losses as low as 2.7 dB m^{-1} [49] were demonstrated. It combines optical

Material	Direct bandgap	Achievable Q factor (10^6)	index contrast	χ_2 (pm V^{-1})	n_2 ($10^{-16} \text{m}^2 \text{W}^{-1}$)	
SOI	×	22	2	0	4.5×10^{-2}	[45]
InP	✓	0.045	≈ 0.3	287	1.5	[46], [47]
SiNOI		420	0.5	0	2.6×10^{-3}	[45], [48]
LiNbO ₃ OI		10	0.7	30	9.1×10^{-4}	[45], [49]
AlNOI		0.8	0.6	4.7	2.3×10^{-3}	[45], [50]
Al _x Ga _{1-x} AsOI	✓ [†]	3.5	1.9	180	2.6×10^{-1}	[51]
SiCOI	×	1.1	1.1	25	3.88×10^{-3}	[52]–[54]
GaPOI	×	0.2	1.6	82	1.2×10^{-1}	[55]

Table 2.1: **Selection of photonic platforms with important properties.**

The index contrast is reported between the substrate and the light-guiding material. χ_2 for the largest crystal axis is reported. Table inspired by [44].

[†] Al_xGa_{1-x}As can change from direct to indirect bandgap that depends on the fraction $x \lesssim 45\%$.

transparency from 350 nm to 5000 nm, second-order non-linearity, piezoelectric, pyro-electric, thermo-optical, and photo-refractive effects in a single material. This combination of many effects can be its main drawback in certain cases. As part of this thesis, we developed SNSPDs integrated on LNOI waveguides[65] (see Figure 5.9).

2.3. Building Blocks of Photonic Circuits

Photonic integrated circuits (PIC) are built from a small subset of building blocks to enable a large variety of possible configurations. For a tapeout at a photonic foundry, a so-called process design kit (PDK) is usually provided that contains a set of building blocks with guaranteed performance properties. In contrast to this, in university cleanrooms, the process frequently needs to be developed or tailored to meet individual requirements. This provides for greater creative freedom, but it also limits the ability to reproduce results.

A summary of common photonic elements is shown in Figure 2.2. The **waveguide** has been discussed before. **Grating couplers** allow to couple light off-chip out-of-plane while **edge couplers** allow the same in-plane. Multiple splitting ratios to connect two waveguides can be realized using a **directional coupler**, **y-splitter**, or an **MMI coupler**. Filters can be realized inline using **photonic crystals** where the transmission function can be engineered. **Ring resonators** can be used to implement frequency-dependent add and drop structures. **Phase modulators** can change the phase picked up during propagation in the waveguide. They are a key ingredient to reconfigurability (see next section). Chrostowski et al. [34] provide a good introduction to silicon photonics design.

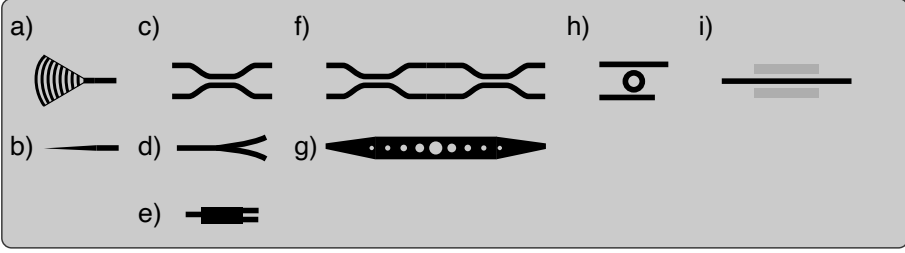


Figure 2.2: **Showcase of waveguide building blocks** a) Grating couplers to couple vertically to a fiber b) Inverted taper to couple to a fiber at the chip facet c) directional coupler for arbitrary splitting ratio d) y-splitter d) Multi-mode-interference (MMI) splitter f) Mach-Zehnder as a tunable beam splitter or modulator g) photonic crystal for engineerable filter or cavity h) Add-Drop filter i) thermal or electro-optical tunable phase shifter

While static circuits can be used to develop many basic applications, it is reconfigurability that allows for a wide range of applications in integrated photonics.

2.4. Reconfigurability of Photonic Circuits

Reconfigurable photonics enables dynamic adjustment of circuit parameters after fabrication. This can be done at very fast timescales (ps) for high-speed modulators, or at slow timescales (ms - s) for compensating fabrication tolerances. There are three types of tunable properties: tunable refractive index, tunable absorption, and tunable physical position. Several techniques exist to use one of these properties for tuning.

Thermal tuning is dependent on the material's thermo-optic coefficient. Local heating changes the refractive index of the material, causing a change in mode propagation that can be utilized to alter coupling or tune resonant structures. It is a dominant technique for tuning integrated photonics to date. The process is slow, and there is a lot of thermal cross-talk to deal with, as neighboring structures get heated as well. The heat generated in the chip makes it difficult to realize it in connection with cryogenic operation, which is required for single photon detectors (see chapter 5).

Electro-optic tuning is dependent on the material's electro-optic coefficients (χ_2 , χ_3). The local applied field changes the refractive index. This is used to create high-speed switches and modulators in materials such as LiNbO_3 . The electro-optic effect is very sensitive and the effective refractive index normally drifts with time. The working point of the device therefore needs to be actively feedback controlled.

Plasma-dispersion tuning is a technique employed widely within silicon photonics for fast modulation of the phase picked up in a waveguide section.

It is based on the principle, that the refractive index within silicon depends on free carriers. By incorporating a P(I)N junction in the waveguide, this parameter can be varied with GHz frequency. The disadvantage is that even in the on-state the loss is quite high, making it non-feasible for on-chip quantum optics. Additionally, the injection of carriers also modulates the loss of the material.

Mechanical tuning is dependent on physically moving elements on a photonic chip. These micro-electromechanical systems (MEMS) use the piezo-electric effect or electro-static actuation to change the physical configuration of a circuit. The change in e.g. the gap of a directional coupler can lead to a change in the coupling ratio (Figure 2.3). The advantage is no heating, stable and repeatable operation, and no specific material properties are necessary. The disadvantage is limited operating speed to low MHz. This makes them an excellent technique used within cryostats and a complementary technique to electro-optics for setting the operating point.

Photonic MEMS are not yet widely employed in large photonic integrated circuits. In demonstrator devices, they have been used for phase shifting in waveguides, or to tune coupling between structures such as resonators and waveguides. The physical movement of waveguides can be used to create switches that connect different ports e.g. to create a large beam steering chip[66]. A recent summary of photonic MEMS can be found in Errando-Herranz et al.[67].

As part of this thesis, we combined superconducting nanowire single-photon detectors (SNSPD) with MEMS photonic circuits for the first time (Paper 1). Read more about the detectors in section 5.5.

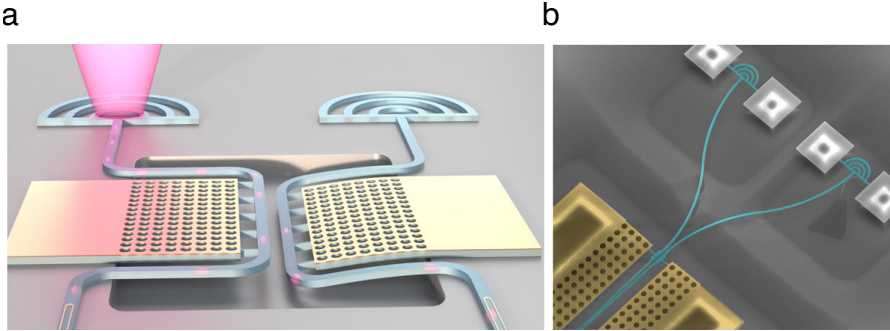


Figure 2.3: **Tunable photonic coupler using MEMS.** a) Artistic illustration of the tuning principle. One waveguide of the directional coupler is bent down using electrostatic actuation. b) False-colored SEM picture of the fabricated device. Waveguides are colored in cyan and the MEMS actuator with electrode region is colored in orange. Adapted from [68] (CC BY 4.0) (Paper 1)

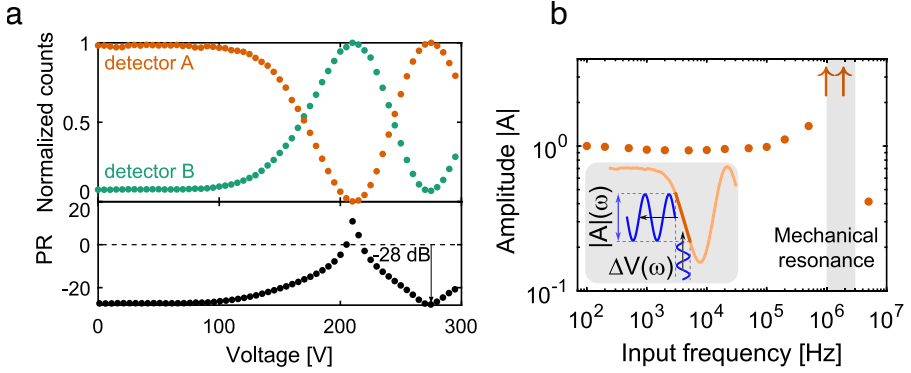



Figure 2.4: **Reconfigurable splitting ratio using photonic MEMS.** a) Tuning of coupling ratio on ports a and b by applying a voltage between electrode and substrate. b) Frequency response of the MEMS switch measured using the SNSPDs. Adapted from [68] (CC BY 4.0) (Paper 1)

We realize a demonstrator circuit containing a directional coupler, that can be tuned by applying a voltage that bends down one waveguide (Figure 2.3a). This changes the coupling distance between the waveguides. To confirm the change in coupling ratio, the light arriving at the two output ports is measured using the SNSPDs. Figure 2.4a shows the detection events on detectors A and B depending on the applied voltage modifying the coupling ratio. The curves are individually normalized, as a fabrication error on detector B limits the effective detection efficiency. Figure 2.4b shows the frequency response of the switch up to ≈ 1 MHz, whereas for higher frequencies the device resonance makes measurements impossible.

2.5. Hybrid Integration on Photonic Circuits

The platforms introduced in the previous section 2.2 fulfill a subset of required properties for individual applications. For example, silicon or silicon nitride are excellent platforms for passive integrated photonics, but their lack of second-order non-linearities χ_2 and low third-order non-linearities χ_3 , as well as the indirect bandgap, make active applications challenging. Ideally, one could combine lasers or single-photon emitters in III-Vs, non-linearities in LiNbO₃, and detectors built from superconducting thin-film NbTiN in the same platform. This is the concept behind hybrid integration; to take the best of all worlds[69].

Nowadays integrating gain material for lasers has been demonstrated on silicon-based photonics[70], Silicon Nitride[71], or LNOI[72]. Lithium Niobate for high-speed modulation has been integrated with silicon[73] and silicon nitride[74]. A review of multiple methods for hybrid and heterogeneous integration can be found in Kaur et al.[75].

Two forms of hybrid integration were demonstrated during this thesis. The first example is the integration of Cu_2O on a silicon photonics platform (Paper 2). Cu_2O or cuprous oxide is a semiconductor that has been investigated early on in semiconductor research[76]. It has a direct band-gap of 2.17 eV (or 571.36 nm ) at liquid helium temperatures[77]. It was Cu_2O that provided early experimental proof for the existence of excitons[78] when initial hydrogen absorption lines were observed up to the principal quantum number $n = 9$ [77]. Due to this history and the existence of large excitonic Rydberg states, it is a material that was over the years used to study fundamental exciton physics[79]. As an early promising candidate for solar cells[80] it could not compete with doped silicon. Nowadays, complementing silicon with a second bandgap material, which promises higher efficiency, revives the material for this use case[81]. The fundamental research has been rekindled by the demonstration of Rydberg states with principal quantum numbers up to $n = 25$ [82] in absorption which was further pushed to $n = 30$ in photoluminescence excitation spectroscopy measurements by Versteegh et al.[83] during the time of this thesis. These Rydberg excitons extend to an estimated diameter of 3 μm . This large diameter promises that experiments usually conducted using Rydberg atoms, such as the Rydberg blockade, can be reproduced in solid-state materials.

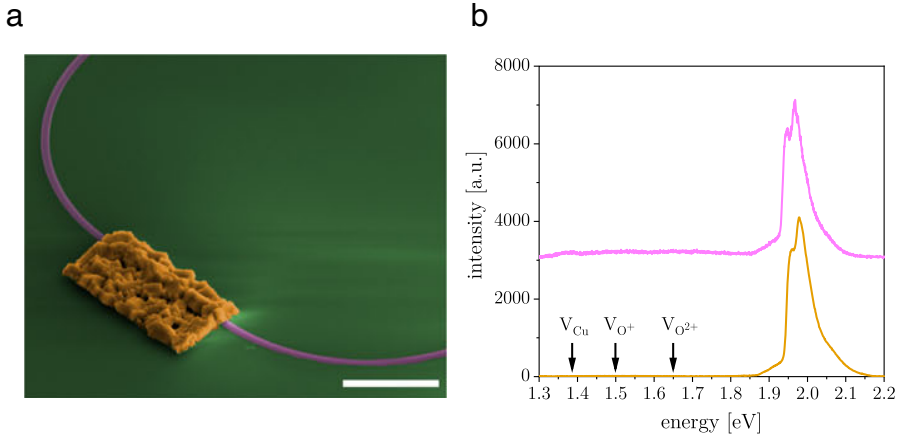


Figure 2.5: **Cu_2O microcrystals coupled to SiN waveguides.** a) False-colored SEM picture of the waveguide structure (magenta) with Cu_2O grown on top of it (orange) scalebar: 10 μm b) Room temperature luminescence through waveguide (magenta) compared with Cu_2O grown on SiO_2 (orange). The arrows mark the luminescence of typical vacancies. Adapted from [84] (CC BY 4.0) (Paper 2)


While multiple methods for artificial growth of Cu_2O exist, thermal oxidation seems to be a promising avenue for defect-free and mono-crystalline

microcrystals[85]. Steinhauer et al. [84](Paper 2) developed a recipe for high purity material that can be co-integrated with silicon nitride (Figure 2.5a). We demonstrate Rydberg excitons in micro-meter scale crystals at mK temperatures[84] and show the coupling of the exciton emission at room temperature to photonic waveguides (Figure 2.5b). The absence of defect-induced luminescence marked with the arrows highlights the quality of the material. We envision the coupling to integrated photonic cavities of high-n Rydberg states e.g. to enhance the interaction with Rydberg blockade-induced non-linearities[86].

The second example is the integration of WS_2 , a 2D material, on silicon nitride to enhance supercontinuum generation within SiN waveguides (Paper 3). 2D materials are a large family of crystalline materials that can be prepared in a planar few-layer form. While the in-plane bonds are strong, inter-layer bonds are of the van der Waals type. This allows access to new material configurations as they can be stacked to form new material combinations. Within photonics, these materials have been used to build light-emitting devices and photodetectors[87]. The integration of 2D materials on waveguides to increase non-linear processes has been reported on several platforms such as graphene oxide, MoS_2 , and GaS .

The chosen material, WS_2 , displays good transparency and shows a strong optical nonlinearity in the telecom wavelength range. It can be prepared by exfoliation from bulk material via a variety of vapor deposition growth techniques. It holds great promise for applications in electronics and photonics, both of which are still in their infancy. Realizing field-effect transistors, photodetectors, light-emitting devices, and modulators were among recent demonstrations[88].

In Paper 3 we use it to enhance the third-order nonlinearity provided by the silicon nitride waveguides for self-phase modulation. Figure 2.6a shows an optical image of the waveguide with integrated flake and Figure 2.6b shows the Raman signal integrated around the 2LA peak of an optical scan over the waveguide. The different intensities show that regions with different numbers of layers exist in the transferred flake.

The waveguides fabricated during this thesis with a thickness of 330 nm and a width of 760 nm show a loss of 1.12 dB mm^{-1} at a wavelength of 800 nm . The loss increased by $\approx 1.35 \text{ dB mm}^{-1}$ (a total of $\approx 2.47 \text{ dB mm}^{-1}$) after integrating a few-layer WS_2 flake. We measure the pulse spectra (I) before the waveguide, (II) after transmission through a 4 mm pristine SiN waveguide, and (III) after integrating a $14.8 \mu\text{m}$ long flake of WS_2 . The enhancement by such a short section is visible in Figures 2.6c and 2.6d for 1.35 kW and 2.7 kW peak power. The pulse broadening observed increases by 48.8 % and 36.4 % for the two powers, because of the integration of the 2D material.

Integrated quantum photonics can also profit from hybrid integration for the generation and detection of single photons. Single photon generation from atomic-like sources is possible via defects within a crystalline substrate e.g. in SiC [90] or Si [91] which allows building waveguides around the emission sites. An alternative approach is to integrate a photon source subsystem. In recent years, quantum dots, nanowires, two-dimensional materials, and emitters based on

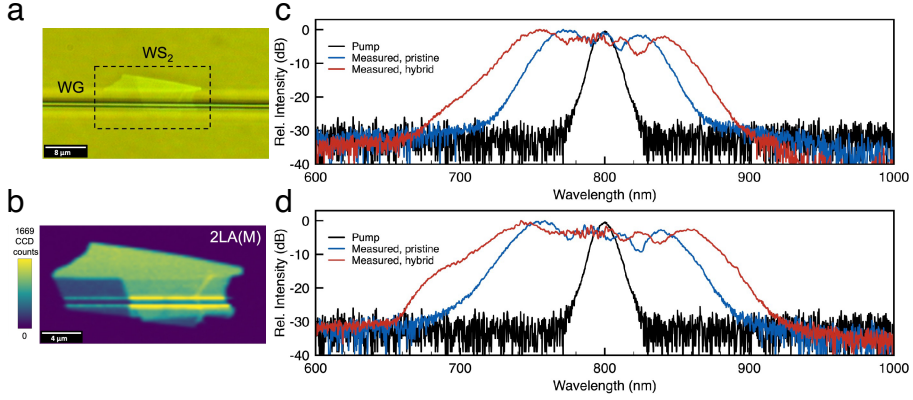


Figure 2.6: **Supercontinuum generation enhancement using a few-layer WS₂ flake on SiN.** a) 2D flake on top of a SiN waveguide. b) Raman signal integrated around the 2LA peak of the flake on top of the waveguide. c) Measured pulse spectra before, after transmission through a 4 mm long waveguide, and after integrating a WS₂ flake at a peak pump power of 1.35 kW. d) as c) but with a peak pump power of 2.7 kW. Adapted from [89] (CC BY 4.0) (Paper 3)

crystal defects have been integrated directly onto photonic waveguides. These efforts have been recently summarized by Elshaari et al.[92].

Work on integrating single-photon emitters was supported during this thesis and is reported by Errando-Herranz et al.[93] and Elshaari et al.[94]. More details on single-photon sources can be found in chapter 3.

To detect light including single photons in integrated silicon photonics, a detector component is required. Because silicon has a weak absorption beyond ≈ 1100 nm another material must be included. One possibility is to make single-photon avalanche diodes (SPAD) by combining germanium and silicon[95]. Chapter 5 discusses an alternative method for single photon detection based on superconducting nanowire single photon detectors (SNSPD).

Creating Single Photons

Quantum Optics

Optical single photons are the building block for quantum information science. Quantum communication utilizes single photons to distribute secret keys, that are protected by the laws of physics. Optical quantum computing uses single photons as the energy running the computation. The generation of single photons usable for these tasks is discussed in this chapter.

This section will provide a brief introduction to individual light particles known as photons. It will go over relevant properties, the setups required to investigate them, and the physical methods available to create single photons.

3.1. Single Photon: What Does It Mean?

Beyond the classical description provided by Maxwell's equation, light can be described as a harmonic oscillator system[2]. While not immediately obvious, this viewpoint allows for the description of modern quantum optics experiments, such as increased resolution through squeezing or access to a new resource: *entanglement*.

The book by Mark Fox[96] provides an introductory treatment and Gerry and Knight[97] supplement any learning outcomes with a more thorough introduction.

We can count the number of oscillation quanta ($E_{\text{photon}} = hc/\lambda$ e.g. 1.282×10^{-19} J for a photon at 1550 nm) in our light state and call it the photon number n . An oscillation eigenstate is then called Fock state $|n\rangle$ and we can describe new states of light through the superposition of multiple Fock states. By classifying a state with the same average photon number by its variance we can identify three types. They are sub-Poissonian with the variance $\sigma_n^2 < \langle n \rangle$, Poissonian $\sigma_n^2 = \langle n \rangle$, and super-Poissonian statistics $\sigma_n^2 > \langle n \rangle$. One example for each type is plotted in Fig. 3.1.

The pure Fock-state $|n\rangle$ is then sub-Poissonian light with an average photon number $\langle n \rangle = n$ but a variance of 0. A single photon ($|1\rangle$) is a sub-Poissonian state with $\langle n \rangle = 1$. The previous few decades have demonstrated that there are numerous methods for producing single photons. We can roughly categorize them into three classes.

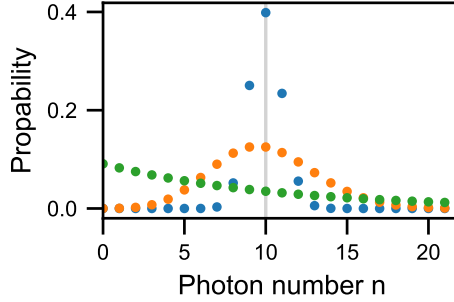


Figure 3.1: **Different photon statistics.** All distributions have a mean photon number of $\langle n \rangle = 10$. A Poissonian distribution is shown in orange, with $\sigma_n^2 = \langle n \rangle$. The sub-Poissonian distribution is shown in blue with $\sigma_n^2 = \langle n \rangle / 10$. The super-Poissonian statistic shown in green here is thermal light (a Bose-Einstein distribution), with $\sigma_n^2 = \langle n \rangle + \langle n \rangle^2 = 110$

The most intuitive way is to **attenuate a laser**, a Poissonian distribution¹, to power values $\langle n \rangle \ll 1$. Due to the variance shrinking with the power of the laser, whenever there is a detected photon, the state likely collapsed to $|1\rangle$, and measurements of $|2\rangle$ and higher are negligibly small. The laser light is said to be within the *single-photon limit*. While this allows for testing single-photon detectors and implementing decoy-state based Quantum Key Distribution (QKD)[98], [99], it does not bring advantages beyond the no-cloning theorem and the brightness of such a source per pulse is limited depending on the application (e.g. $\langle n \rangle \approx 0.5$ for QKD[100]).

A second way is using a **non-linear process** such as spontaneous parametric down-conversion (SPDC) discovered in the late sixties[101], [102]. This method is the workhorse for quantum optics experiments and applications today as bright single- and entangled photon sources[103]. By interacting with vacuum through the non-linear material, a photon from the pump laser is converted into two photons known as signal and idler. Because the creation is spontaneous and its likelihood decreases with increasing photon number, a signal with very low two and more-photon content can be produced. The high single-photon flux generated by higher pump power increases the possibility of two-photon states, which is a tradeoff for these types of processes. If only one photon is required, the second photon can be used to signal the creation of the first. Schemes using multiplexing and post-selected routing of photons show promising future developments for increased brightness and deterministic generation[104].

A third way is to create a single photon through **spontaneous emission** of a system with atomic-like transitions coupled to the electromagnetic field. The system can be of multiple kinds such as calcium atoms, the first system

¹Using a super-Poissonian light source (e.g. thermal light) shows bunching behavior, leading to likely having bunches of photons, even at low intensities.

demonstrating single-photon emission[105], or defects within crystal structures such as NV centers, used to demonstrate a loophole-free bell-test[106], or confinement effects by changing the material properties on larger length scales, such as self-assembled quantum dots, the purest single-photon source to date[107]. A summary of various single-photon sources with a focus on quantum dots is given by Senellart et al[108].

The emission from systems based on spontaneous decay is the focus of this thesis and several atomic-like systems are discussed in sections 3.5, 3.6, and 3.7.

3.2. Single Photons: What Do We Want?

The goal of using single-photon sources based on spontaneous emission in quantum information applications leads to a wish list of characteristics[109] (shown in Figure 3.2) that must be met to succeed. When a photon is requested for some application, an ideal source will emit identical photons every time (Figure 3.2a). In practice, the source will be unable to deliver on this promise in several ways.

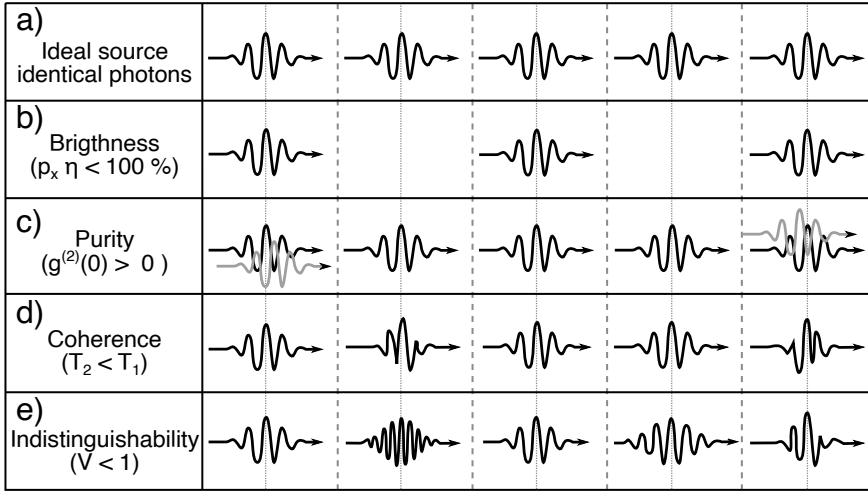


Figure 3.2: **Photon properties wishlist.** a) ideal source of identical photons that are generated with each excitation event. b) A brightness smaller than 100 % leads to empty timeslots because of non-unity generation (p_x) or loss of photon after emission (η). c) Some excitation events lead to more than one photon. d) The phase within the emitting system is not stable until the photon is emitted e) Subsequent photons are not identical due to e.g. spectral changes. Adapted with permission from [109, Fig 3.1].

If the source sometimes does not produce a photon this will reduce the brightness of the source (Figure 3.2b). The reason can be e.g. loss during

extraction, inefficient excitation, or non-radiative decay. Such a source, which is the common case in experiments today, increases the complexity and run time for quantum optics experiments and applications.

The generated photons should always be a single one. This is necessary if the state is used as input for further computing or the achievable rate of the protocol depends on it[110]. The behavior is verified using a Hanbury Brown and Twiss (HBT) measurement[7], discussed in section 3.4. The measurement outcome summarized in the $g^{(2)}(0)$ value should be as close as possible to zero (Figure 3.2c).

The coherence of the system (Figure 3.2d) is characterized by the phase stability (T_1) of the state compared to its lifetime (T_2). If the phase of the system is lost before the photon is emitted this leads to different spectral shapes of photons on every emission. This makes subsequent photons distinguishable.

The indistinguishability (V) (Figure 3.2e) is a property that combines several other properties. It requires a high purity, and a long coherence time but while the other properties were only interacting with the emitted photon itself, indistinguishability connects subsequent photons. High indistinguishability describes the similarity between photons emitted by a source. It is measured using the Hong-Ou-Mandel effect[9], where identical photons leave a beamsplitter always on the same output port.

Other desirable properties are entangled photon generation[111] or coherent memory[112] within the system. While individual goals have been met for various systems, combining many or all of them into an experiment or device is for most if not all systems still a work in progress.

3.3. Photoluminescence Setup. Extracting Single Photons

The single photons investigated in this thesis, are emitted after the absorption of photons often provided by a laser. This process is called photoluminescence (PL). The light is generated from sub-micron material features. This requires the collection area to be confined to avoid contamination by neighboring emission sites. Such a setup is called μ -photoluminescence (μ -PL), in contrast to other types of photoluminescence that measure bulk properties of the investigated material. The small collection area is achieved through a high-NA objective or lense creating a small spot on the sample used for collection.

A typical setup configuration is shown in Figure 3.3. A laser, either pulsed or continuous wave (CW) is power controlled and then through a beam-splitter or dichroic mirror coupled into the detection path. The beam-splitter can be polarizing or has a 90:10 ratio to direct as much of the generated signal to the detection output port. The laser is then focused through the so-called "first-lens" (often a high-NA objective) onto the sample. Ideally, a diffraction-limited spot is created. The emitted signal is collected by the same lens and leaves the beam splitter mostly through the high-efficiency port. The signal is now either coupled to a fiber or free-space directed on a slit and measured using a high-efficiency spectrometer with a cooled CCD or linear array detector.

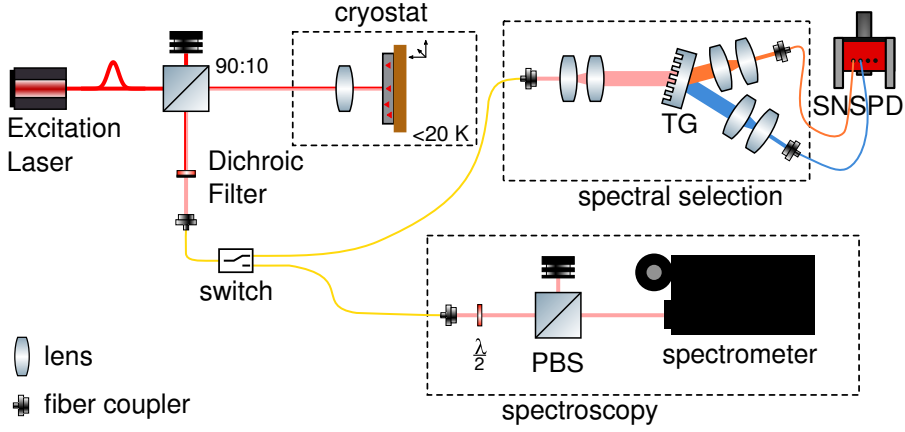


Figure 3.3: **Typical photoluminescence setup** The sample is mounted inside a cryostat or at room temperature (not shown) on a movable stage ($\hat{x}, \hat{y}, \hat{z}$). An objective or lens is used to collect the light from the sample. An excitation laser (pulsed or continuous-wave) is coupled through a beamsplitter (often with a ratio of 90:10) into the collection path of the setup. After optional filtering of the laser using a dichroic filter, the detected light is coupled to a fiber providing the angular selectivity for a confocal arrangement. The signal is then either sent to the spectroscopy setup or spectrally filtered for single-photon detection. The spectroscopy setup consists of a rotatable $\lambda/2$ waveplate and a polarizing beam-splitter (PBS) to allow for polarization-dependent spectroscopy. The spectral selection is e.g. performed using a transmission grating (TG) that allows for two lines to be selected and coupled into fibers for single-photon detection using SNSPDs. The drawing is created using the ComponentLibrary by Alexander Franzen (CC BY-NC 3.0).

Many of the single-photon emitters in solid-state are strongly coupled to the environment and are therefore disturbed by phonons in the host material. Therefore they often require cryogenic refrigeration. While some systems such as defects within crystals still emit single photons, even if with degraded properties, other systems e.g. self-assembled quantum dots with comparatively low trapping potentials no longer emit single photons as the transitions are washed out. Figure 3.3 shows a dashed box for the possible cryostat, with multiple operating temperatures from 20 K down to 150 mK.

To measure single photons on single-photon detectors, first, an individual emission line needs to be selected, as many real world systems have several possible radiative transitions and background luminescence. Several options for filtering exist such as a band-pass filter that coarsely selects a region, an in-house build transmission spectrometer[113], an inline fiber filter (Koshin Kogaku, FBPF), or coupling the reflection of a notch filter (Optigrate, BragGrate)[114].

3.4. HBT-Measurement. Proofing Single Photon Character

A spectroscopic measurement can deliver excellent clues towards the origin of an emission line through power-dependent[115] or polarization-dependent measurements[113], [116]. This can indicate that the line is single-photon in nature.

A more definitive proof for single-photon emission is based on the Hanbury Brown and Twiss (HBT) measurement. Initially invented to measure the angular size of stars[6], it was used by Kimble et al.[7]. to show the single-photon character of emitted photons from sodium atoms.

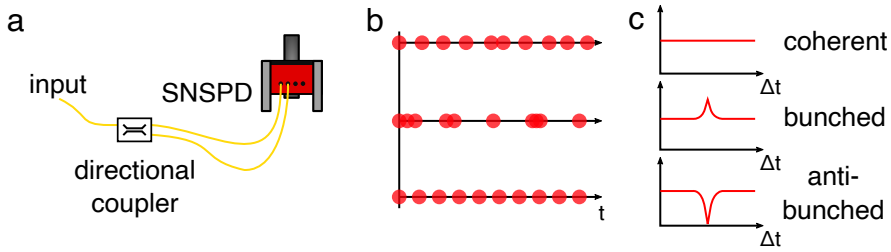


Figure 3.4: **Hanbury Brown and Twiss (HBT) measurement.** a) typical setup of an HBT measurement consisting of an input port that is split (mostly 50:50) and the output ports, that are connected to two single-photon detectors. For a single-photon source, the photon needs to leave through one of the two ports, leading to an anti-bunched correlation measurement. b) Time-trace of photons emitted by a coherent, bunched, and anti-bunched source. c) Sketched correlation histogram for each type of source.

A typical setup is shown in Figure 3.4a. The input signal is sent on a beam-splitter (e.g. a directional fiber coupler) and the output ports are connected to a single-photon sensitive Geiger-counter-like detector. An excellent detector of this kind is discussed in chapter 5. The arrival time of the photons on the two detectors are correlated and the absence of detection events at the same time proves that no multi-photons are impinging on the beam-splitter. The probability of detection events at the same time is called the single-photon purity with an ideal value of 0 and a record value for single-photon emitters of $g^{(2)}(0) = (7.5 \pm 1.6) \times 10^{-5}$ [107].

The same setup can not only prove the single photon purity of a light field but e.g. estimate the temperature of the dark body emitting the light. For further reading, Baym[117] wrote a detailed review of the capabilities of HBT measurements.

Knowing how to verify a single photon emitter, we next highlight three types of single photon sources investigated during this thesis.

3.5. Crystal Defects: Single Photon Sources

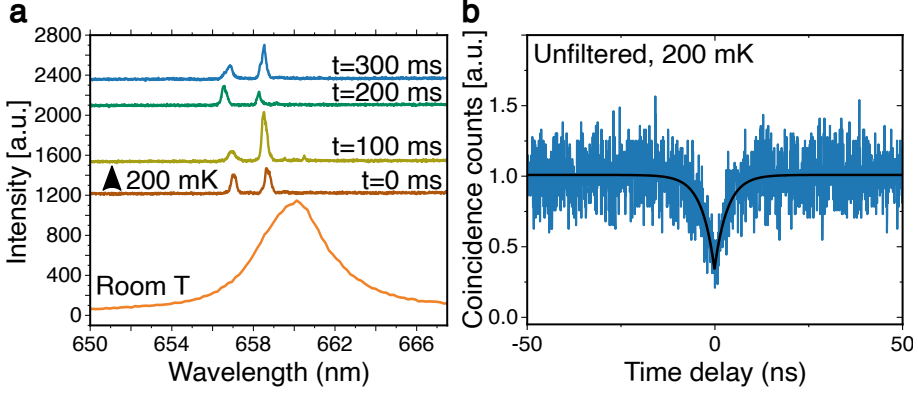


Figure 3.5: **Single-photon emission from defects in hBN.** a) Spectra of single-photon emission of the same emitter at 200 mK and room temperature. The time series of spectras shows the different transitions, only visible at cryogenic temperatures. b) HBT measurement of single-photon emitter at 200 mK with a multi-photon probability $g^{(2)}(0) = 0.33 \pm 0.03$. Data reported in [118] (Paper 4).

For a long time, crystal (point) defects or color-centers have been utilized as promising single-photon emitters. Vacancies within the lattice and foreign atoms provide local optically active transitions that emit single photons on decay. The NV-center, a nitrogen-vacancy defect within diamond is the most studied. Notable other defects exist in diamond[119], silicon carbide[120], and silicon[91].

In **Paper 4** we investigated crystal defects within hexagonal boron nitride. hBN is material available as bulk (several layers) and mono-layer. hBN itself is most widely spread as the ideal substrate to transfer other 2D materials like graphene to, but it also is researched as a photonic material. Non-linear optics and photon emitters within hBN promise a wide area of applications. The emitters can emit a room temperature from 570 nm to 750 nm and are usually bright, optically stable, and linearly polarized. They can be tuned via strain or electric field, and their location within monolayers, nanocrystals, or bulk layers simplifies their integration with other platforms. This has been used to embed them in 1D photonic nanobeam cavities or spin coat them on a chip and couple them randomly to waveguides [119], [121].

In this work, we thermally activate the emitters in h-BN nano-crystals that are drop-casted on a SiO₂ on Si substrate with alignment markers. In Figure 3.5a one can see a typical luminescence of the same emitter at room-temperature

and at 200 mK. We observe an FWHM of 3.75 nm at room temperature that decreases to 0.27 nm at 200 mK. Additionally, we observe spectral wandering of the emitter at cryogenic temperatures that is hidden within the broadened room temperature emission. We measure a single-photon purity at 200 mK of $g^{(2)}(0) = 0.33 \pm 0.03$ by only filtering the laser. We encapsulate the characterized emitters within SiO_2 below a silicon nitride slab and etch waveguides around pre-selected emitters to demonstrate the coupling of the emitter to the waveguide.

3.6. 2D Materials: "Single-Layer" Quantum Dots

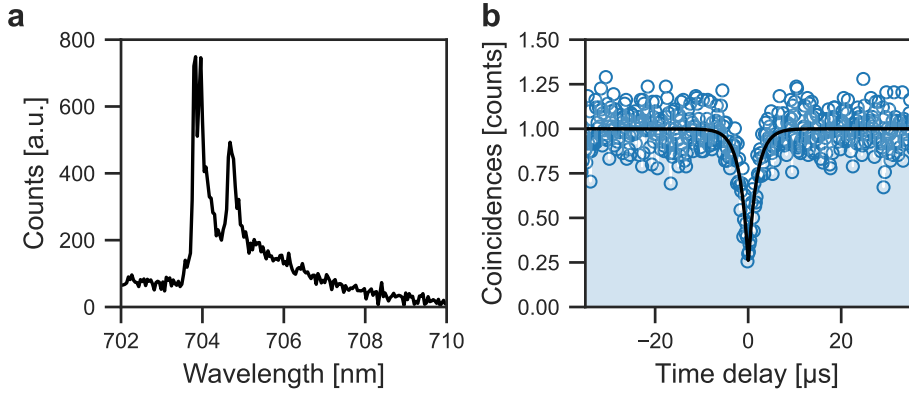


Figure 3.6: **Single-photon emission from MoS₂** a) Emission spectra of a He-FIB induced defect hosted within MoS₂ at ≈ 5 K. b) Measurement of single-photon character of the zero phonon line (ZPL) with a $g^{(2)}(0) = 0.24 \pm 0.04$. Data reported in [122] (Paper 5).

The second class of emitters is located within mono-layer crystalline materials, often called 2D materials. In recent years a plethora of suggestions for applications and new physics with 2D materials were proposed[87], [123], [124]. The ability to stack different kinds of layers allows for a LEGO-like playground[125], creating artificial new materials. After several groups[126]–[129] reported on single-photon emitters in WSe₂ in 2015, numerous 2D material systems creating single-photon emitters were discovered. There are various types of formation principles, such as strain-induced or defect-induced emitters (similar to the discussion in the previous section). A recent review article[130] summarizes the developments and challenges in the field.

An exceptional example of the latter kind is the emitters reported in MoS₂, as they can be created using a lithographic method based on focused Helium Ion Beam irradiation [29]. Their emission (Figure 3.6a) is centered around 708 nm ■ (1.75 eV) and is attributed to sulfur vacancies[131]. This technique allows to position control more accurately than other system, which

can be used to accurately create an emitter at the location of e.g. waveguide coupling structures, existing emitters, or cavities. While initial proof of single-photon emission was limited to power-dependence studies[29], part of this thesis was the first successful HBT measurement with a single-photon purity $g^{(2)}(0) = 0.24 \pm 0.04$ (Figure 3.6b) from this type of emitters reported in [122] (Paper 5).

3.7. Quantum Dots: Large Scale, Artificial Atoms

Optically active quantum dots are hosted within a semiconductor bulk material, that is locally replaced by a different type of semiconductor with a smaller bandgap. The different bandgaps form a local trap for excitons and create transitions similar to an atomic system. This is why they are often called artificial atoms. The control over material and shape of the inclusion allows for designer freedom in emission properties such as wavelength. The most successful material systems are III-V semiconductors such as InAs/GaAs[132], InAs/InP[133] or InAs/(InGaAs/GaAs)[134].

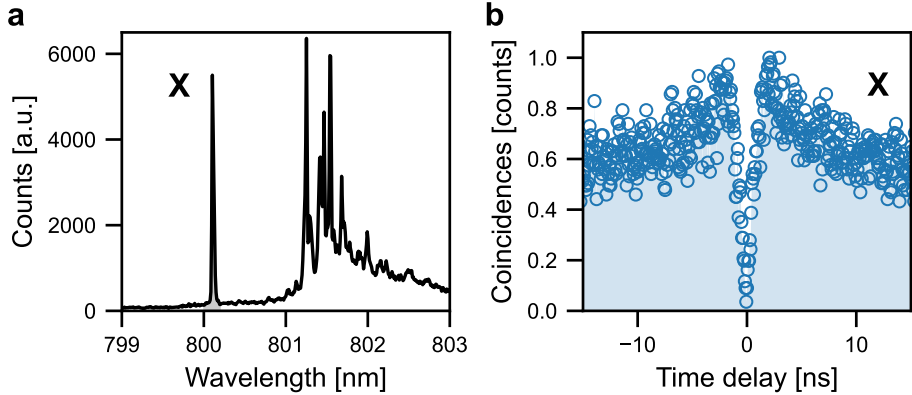


Figure 3.7: **Single-photon emission from a self-assembled QD.** a) Emission spectra of a QD excited above-band at $\lambda_0 = 632.8$ nm at ≈ 200 mK. The exciton transition (X) is marked. b) Proof of single-photon emission of exciton transition (X) through an HBT measurement.

Single-photon emission[135] and indistinguishable photons[136] generated by quantum dots were already demonstrated around the turn of the millennium. Since then the field has worked on improving fabrication and measurement techniques to produce the cleanest[107] and almost identical[137] single photons. Quantum dots can be tuned through various methods such as electric field, magnetic field, and strain. This allows for compensation of fabrication variability. Furthermore, polarization-entangled photon pairs can be created through a radiative cascade. Overall they provide at various wavelengths bright, pure and

indistinguishable photons. They are very mature single photon emitters in the solid-state, similar to diamond defects, and may be ready for applications such as quantum communication[138] and quantum computation soon. A recent review by Senellart et al.[108] summarizes the field.

Figure 3.7a shows a typical photoluminescence spectrum of a quantum dot emitting at ≈ 800 nm [139] excited with a CW-laser ($\lambda_0 = 632.8$ nm) at ≈ 200 mK. The exciton transition is marked and an HBT measurement is shown in Figure 3.7b demonstrating pure single-photon emission. As part of this thesis, quantum dots at telecom wavelength were used to demonstrate the generation of entangled single photons (Paper 7) and modify their spectrum using phase modulators (Paper 6) (see Section 4). Quantum dots at 795 nm were used as a single-photon source to couple to integrated photonic circuits in Paper 1 (section 5.5).

Manipulating Single Photons

Quantum Optics

After decades of research have been devoted to developing the ideal emitter or detector, they are becoming commercially available. Similar to lasers and photon detectors, which were once considered research objects, that now serve as a basis for a wide variety of scientific and industrial applications. Quantum optics' future lies then in the manipulation of quantum states of light. Two examples are the photonic quantum computer and building a quantum internet. The quantum computer works based on detecting single photons after them propagating through a mesh of tunable photonic circuits[140]. Connecting multiple quantum computers to networks[18] will need the combination of multiple technologies, such as photon sources, quantum memories, and communication fibers[18]. This requires to frequency convert[141], [142] the photons at different stages in the network or adapt their temporal shape[143].

While much of the work in this thesis has been focused on light creation (chapter 3), guiding (chapter 2), and detection (chapter 5), this chapter will explore a small excursion of manipulating single photons. It begins with altering photons after they have been emitted using electro-optic modulation, then move on to modifying photons before they have been emitted by tuning the source using strain.

4.1. Electro-optic Modulation for Single Photons

While the technologies for frequency conversion between larger wavelength regions (e.g. 800 nm to 1550 nm) are based on non-linear processes, a different way to finely tune an emitters wavelength or photon shape is to modulate its phase. This can be done using acousto-optic or electro-optic modulators. Schemes utilizing the second, have been used to shift single photons by 25 GHz[144]. Recent proposals show a similar technique could be used to remove the fine-structure splitting of a quantum dot[145].

As quantum communication protocols such as the quantum repeater depend on the Hong-Ou-Mandel effect, the interacting photons must be indistinguishable (see also section 3.2). While in atom-based sources multiple atoms of the same kind emit indistinguishable photons[146], solid-state sources show a spread in emission wavelength and lifetime. When connecting multiple sources in

the future they will need to be brought into resonance and fine-tuning of their photon properties is necessary. This can be achieved e.g. using strain tuning, temperature tuning, or electric field tuning. More dynamically and for multiple emitters on the same sample, this can be achieved through optical modulation[147].

One way of optical modulation is based on the electro-optical modulator to modify the spectral shape of a single photon. With the Pockels effect, the application of an electro-magnetic DC or RF field changes the local refractive index and thereby imprints a (time-dependent) phase shift on the signal. This technique is extensively used in optical communication, where data is transmitted via a light carrier. A phase modulator is then the basic component for more sophisticated modulator devices, such as an amplitude modulator or an IQ modulator, which control the carrier's amplitude and phase.

In the simplest experiment, the phase modulator is driven by a sine signal and moves the energy of the central signal, called the carrier, at a wavelength λ_0 to wavelengths around it, called sidebands, each of them separated by the frequency of the modulation. By creating more complex signals e.g. a sawtooth-shaped signal all the energy of the original signal can be shifted to a new wavelength (serrodyne modulation)[148], [149].

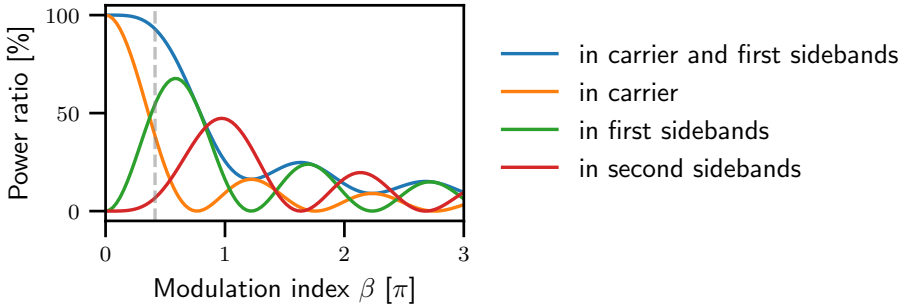


Figure 4.1: **Power ratio in sidebands after phase modulation.** The power ratio in carrier and sidebands depends on the modulation index. The vertical grey line marks the operating point for the result at 26.5 GHz in Paper 6.

This behavior can be understood by looking at a complex exponential signal $y(t) = \exp(i\omega_0 t + i\varphi(t))$ modulated with a time-dependent phase $\varphi(t) = \beta \sin \Omega t$, where ω is the angular frequency of the original signal, Ω is the angular frequency of the phase modulation and β is called modulation index and defines how much the phase of the signal is shifted. By using the Jacobi-Anger expansion

on this function, we obtain

$$\begin{aligned} \exp(i\omega t + i\beta \sin(\Omega t)) &= \exp(i\omega t) \left(J_0(\beta) \right. \\ &\quad \left. + \sum_{k=1}^{\infty} J_k(\beta) \exp(ik\Omega t) + \sum_{k=1}^{\infty} (-1)^k J_k(\beta) \exp(-ik\Omega t) \right) \end{aligned}$$

where J_k are the Bessel functions of the first kind of order k . The J_0 term is describing the carrier, the remaining non-modified signal, while the individual sum terms containing J_k are the k sideband with an increased (decreased) frequency by $\frac{\Omega}{2\pi}$. Figure 4.1 shows the power in the carrier, the first and the second side-bands for a varying modulation index β . The leakage into higher side-bands can not be eliminated for phase modulation with a sine driving signal, but more advanced modulation schemes can create only two bands[144].

This technique could be utilized to build qubits in frequency space[150]. This has several advantages, such as that their entanglement is not influenced by polarization drifts, the available space opens from just two bases ($|H\rangle$ and $|V\rangle$) to the whole frequency spectra ($|\omega\rangle$) that can be densely packed. Based on single photons generated using quantum dots such qubits could be created.

During this thesis we investigate the compatibility of our quantum dots emitting at telecom wavelengths (Figure 4.2a) with telecom equipment (**Paper 6**) and measure the photon statistics of the side bands created by such a phase modulator. It has been shown that photons of a quantum dot stay indistinguishable even after being modified by a phase modulator[151]. We modulate the emitted single photons similar to the experiment of Paudel et al.[151] and create sidebands next to the main carrier signal (Figure 4.2b). We then spectrally filter these sidebands and measure a cross-correlation between the two channels (Figure 4.2c).

The generated sidebands by phase modulation with a sinusoidal driving signal at multiple frequencies can be seen in Figure 4.3a.

With a modulation index of $\beta = 0.41\pi$, 54.6 % of the photons are shifted into the first-order sidebands, while 7.1 % of the photons are shifted to higher-order sidebands. It is visible that the ratio between the center peak and the side peaks is dependent on the frequency. This is due to the non-linear frequency response of the applied power for the signal generator and amplifier. A higher modulation index shows that more RF power arrives at the modulator, and it ranges from $\beta = 0.41\pi$ to $\beta = 0.57\pi$ in this experiment.

We evaluate the single-photon purity by performing an HBT-type correlation measurement on the two sidebands (Figure 4.3b) with a result of $g^{(2)}(0) = 0.16 \pm 0.06$. The phase modulator behaves like a beam-splitter but in frequency space and creates a superposition of the single photon, in first approximation, in the carrier, the upper, and the lower sideband.

One thing that became quite apparent during these experiments was the substantial losses that are still present in traditional telecom equipment. There is currently no pressing need in the industry to reduce these losses, but when

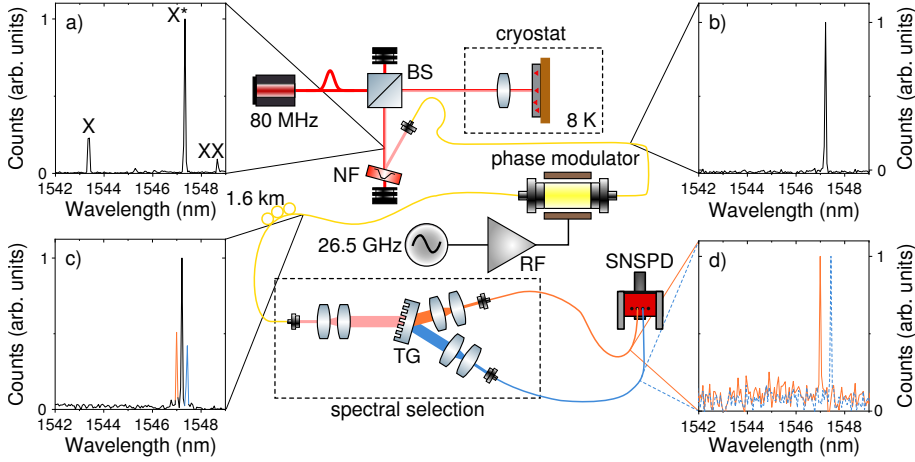


Figure 4.2: **Sideband creation using a phase modulator.** a) Emission of exciton (X), biexciton (XX) and trion (X*) single-photons in the telecom C-band. b) Selection of the trion using a notch filter in reflection. c) Sideband generation through sinusoidal phase modulation. d) Filtered single photon channels connected to SNSPDs for cross-correlation measurements. Reproduced with permission from [114] under OSA Open Access License. The drawing is created using the ComponentLibrary by Alexander Franzen (CC BY-NC 3.0).

quantum networks become more widely implemented, products will follow that provide low insertion loss and make a combination of active fiber equipment and single photons a powerful tool for quantum optics.

4.2. Fine-structure Tuning using Strain

Epitaxially grown semiconductor quantum dots are excellent single photon sources (see section 3.7), that support the generation of polarization-entangled photon pairs by a radiative cascade (Figure 4.4a). The optical excitation pulse creates two excitons ($|XX\rangle$) through a resonant or non-resonant path. Then the first photon emission leads through two paths with opposite polarization to an ideally degenerate exciton level ($|X\rangle$) which then leads to the emission of a second photon. These two photons are maximally entangled in polarization[152] and can be written as the Bell state

$$\psi^+ = \frac{1}{\sqrt{2}}(|HH\rangle + |VV\rangle)$$

where H and V denote horizontal and vertical polarization. Inhomogeneities in material, growth, and strain lead to a slight energy mismatch of the two "indistinguishable" decay paths, the source of the entanglement. This leads to

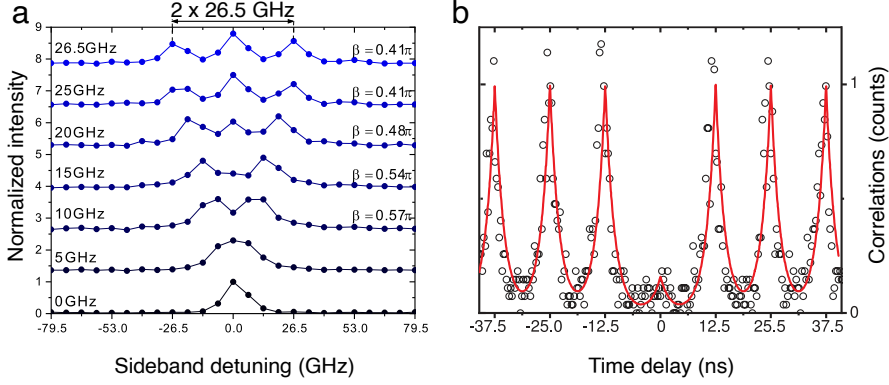


Figure 4.3: **Sideband creation and cross-correlation** a) Tunable sideband spacing based on driving frequency. The varying modulation index β is shown alongside each trace. b) Cross-correlation measurement between the sidebands demonstrating low multi-photon probability. Adapted with permission from [114] under OSA Open Access License.

a time-oscillating entangled state [109]

$$\psi^+ = \frac{1}{\sqrt{2}}(|HH\rangle + e^{i\tau FSS/\hbar} |VV\rangle)$$

where τ is the lifetime of the exciton, FSS is the fine-structure splitting, and \hbar is the reduced Planck's constant. This state can only be utilized with a high fidelity through time-resolution that resolves the oscillating correlations at a period of $T = \frac{\hbar}{FSS}$, h is Planck's constant. The FSS is especially detrimental if one wants to work with photons from two different quantum systems. As the usual protocols depend on the HOM effect, photons must be highly indistinguishable, which is no longer the case if two photons from different emitters with FSS interfere as the phase picked up while being in the exciton state will be random.

Several techniques have been used to remove the FSS such as applying magnetic field, using electric field, the optical stark effect, or applying anisotropic strain [109]. With the last method, through full control of the in-plane strain tensor, it has been shown[153] that the fine-structure splitting can be eliminated while controlling the emission wavelength.

As part of this thesis (Paper 7), we used such a triaxial piezo actuator (see Figure 4.4a) to correct the fine-structure splitting in quantum dots emitting in the telecom C-band [155]. We achieved values as low as $FSS = 1.1 \mu\text{eV}$ resulting in an oscillation period of $(3.9 \pm 0.5) \text{ ns}$. In a second step (Figure 4.4b), we investigate the influence of the time resolution of the single-photon detectors on the maximal achievable concurrence (an entanglement figure of merit) and show that in the low FSS case we can use a bin size of 2.048 ns and still maintain a concurrence value above 50%.

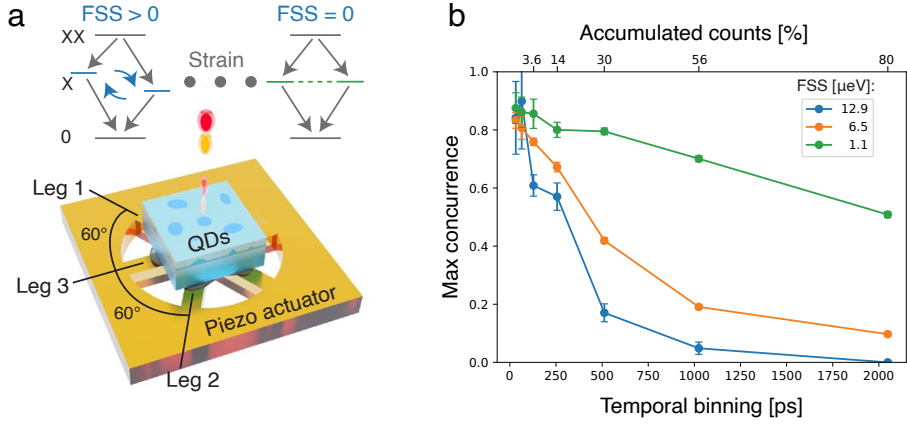


Figure 4.4: **Fine-structure tuning and concurrence measurements.** a) A six-legged actuator is used to fully control the strain applied to the QD sample. b) Concurrence levels achieved for different fine-structure splittings and variable temporal binning. Adapted from [154] (CC BY 4.0)

Detecting Single Photons

Quantum Optics

For many millennia, humans relied only on their own eyes to detect photons. Only the early 18th century discoveries of photosensitive materials and their application to scientific research and photography allowed for the temporary and eventually long-term fixation of light on film by the 1830s[156]. With the development of the photo-multiplier tube (PMT) at the end of the 1930s, 100 years later, we were able to detect individual single photons in the near-infrared and visible wavelength range. Many technological options based on photomultipliers, semiconductors, and superconductors have been developed since then[157]. Within these device classes, a wide range of options is available to provide solutions for scientific and industrial applications. While applications requiring the detection of single photons are still primarily limited to quantum optics research, photon starved measurements use the same instrumentation and make these detectors immediately useable. Light ranging (LIDAR) measurements[158], optical time-domain reflectometry to measure interfaces and defects in fibers[159], and defect detection in semi-conductor production are a few examples[160]. In biological research and industry, DNA sequencing[161], single-molecule spectroscopy[162] and fluorescence correlation spectroscopy (FCS)[163] are techniques utilizing single-photon detection.

This chapter will discuss a wishlist for the perfect single-photon detector. It will introduce superconducting nanowire single photon detectors (SNSPD) and discuss their properties and different technical implementations.

5.1. Requirements for Single-Photon Detection

Detection efficiency is one of the most critical parameters, with a target value of 100 %, that is heavily dependent on the wavelength being measured. **Noise**, also known as dark counts in this context, is an equally important metric, as a relatively low detection efficiency can often be compensated for by a high signal-to-noise ratio (SNR). 0 cts/s is the ideal value. A common way of characterizing this is noise-equivalent power (NEP). The level of signal power that leads to equally many noise detections as signal photons in half a second. **Timing resolution** or **jitter** depends very much on the problem at hand. Ideally, it would be infinitely high, with no uncertainty in the measured

time. The minimum distance between subsequent photons to be detected is limited by the **reset time**. The maximum brightness of the signal that can be detected is then limited by the **maximum count rate**. While the reset time influences the maximum count rate, other bottlenecks such as digital interfaces can also limit it. Combined with noise, the maximum count rate defines the **dynamic range** of the detector. A wide dynamic range allows the detection of the faintest signal while remaining operational in the presence of a bright signal. Closing the gap of measurable photon flux between Geiger-counter and photocurrent detectors would be a useful property for calibration, which could then be traced back to a single photon but one could also envision combined systems of single-photon detectors and photodiodes to increase the dynamic range. **Energy resolution** and **multi-pixel** imaging capabilities are other beneficial properties, as are **energy consumption** for device operation and footprint.

In this thesis, I will concentrate on the superconducting nanowire single photon detector (**SNSPD**), which has probably been the most successful candidate in ticking many of the boxes. The most significant disadvantage is the cryogenic operation, which consumes a lot of energy and has a large associated installation footprint.

5.2. Superconducting Nanowire Single Photon Detectors (SNSPD)

Superconducting nanowire single photon detectors (SNSPD) are the workhorse for single-photon detection within research. They excel in most of the requirements outlined in the section above with small trade-offs when selecting the required parameters. Companies have demonstrated jitter values around 15 ps in close-to-unity efficiency devices at telecom wavelengths (1310 nm)[164], while research groups demonstrate record values of a jitter < 3 ps[165] and a system detection efficiency > 98 % [166].

The initial discovery in 2001 [167] was an electrical response of a superconducting nanowire to single photons inspired by demonstrated light detection in superconducting devices back in the seventies[168]. The research field developed fast as highlighted in Fig. 5.2, with the first fiber-packaging reported in 2006 [169] and SNSPDs integrated on photonic chips in 2011 [170], [171]. The first big step in packaged detection efficiency was up to 28 % in 2010 [172]. In 2013 the 90 % boundary was broken [173] based on the new SNSPD material WSi[174]. The latest values are up to 98 % [166] at 1550 nm. During this time the field investigated multiple material systems. The initial demonstration of photon detection in each system is shown below the timeline in Fig. 5.2. With NbN, NbTiN for (poly)crystalline and WSi, MoSi for amorphous materials, four dominant film materials are currently widely used. Careful material and fabrication engineering led to the discovery of single-photon detection within micro-meter wide bridges in 2018 [175] opening a promising avenue for scaling up and further detector development (see section 5.4).

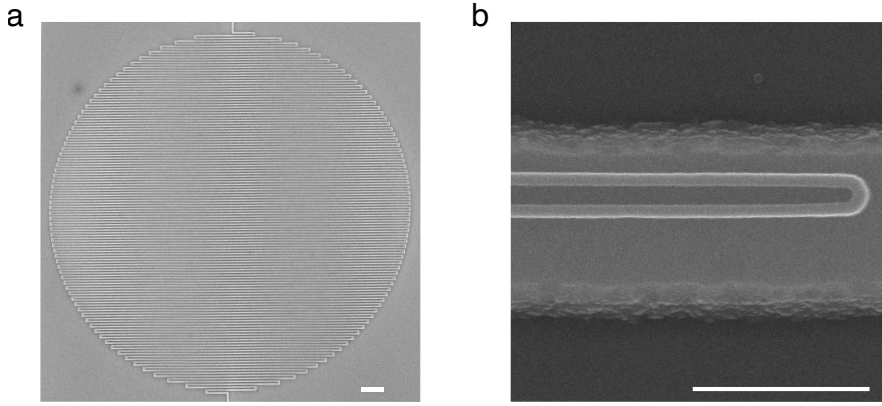


Figure 5.1: **The two most prominent SNSPD designs** a) A meandering SNSPDs for coupling to a fiber allowing almost 100 % **system** detection efficiency. b) A hairpin SNSPD evanescently coupled to a waveguide, allowing for almost 100 % **on-chip** detection efficiency. The scale bars are 1 μm long.

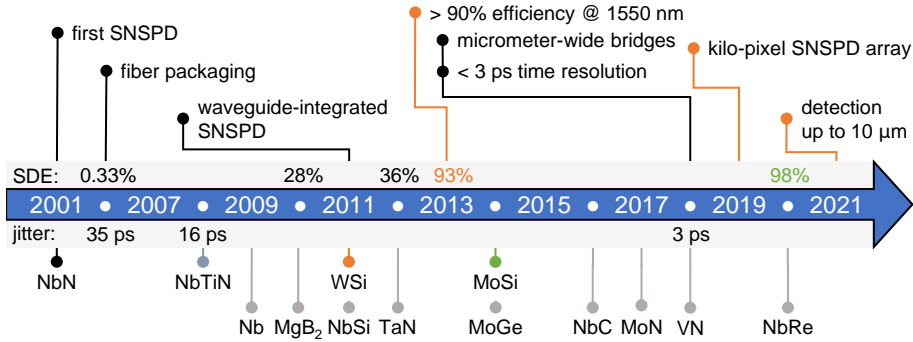


Figure 5.2: **Timeline of the development of SNSPDs.** Above the timeline are important milestones that are colored according to the material system that was used to achieve them. Above and below the timeline, the development in detection efficiency at 1550 nm and jitter values are shown. Materials used to demonstrate operating SNSPDs are shown below the timeline. The colored materials are the most widely used. Reprinted from [176] (CC BY 4.0)

The detection principle was first described using a macroscopic theory[167], [168], which is still used as a simple explanation today. The stages of a single photon's detection are depicted in Figure 5.3.

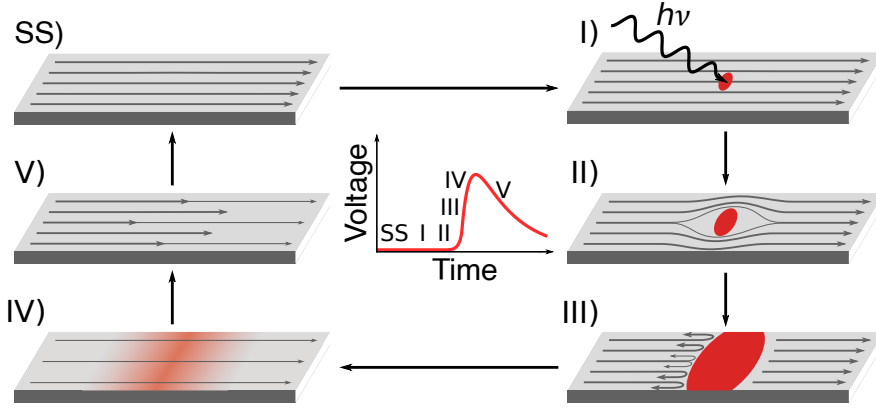


Figure 5.3: **Macroscopic detection processes** SS) The nanowire is initially in a steady-state, biased close to its critical current. I) The absorption of a single photon leads to energy being deposited into the nanowire. II) This energy creates a non-superconducting spot, redirecting the super-current around it, thereby exceeding the critical current in the remaining superconducting area. III) The change in impedance of the so-called hotspot leads to a reflection of the current, generating a high-frequency voltage pulse that signals the photon detection. IV) The reduced current and the heat dissipation into the substrate allow the nanowire to recover superconductivity. V) The bias current restabilizes, thereby increasing the detection efficiency for the next photon. This ends the dead-time of the detector and the device is ready for the next photon detection. Inset shows the timing of each step with respect to the voltage output. Reprinted with permission from [177]. Adapted with permission from Allmaras et al., Nano Lett. 20, 2163–2168 (2020). Copyright 2020 American Chemical Society.

In **Steady State (SS)** the tens-of-nanometer wide superconducting wire is current-biased. The absorption of single or multiple photons in step **I** causes the local breaking of Cooper pairs, which leads to the diversion of the remaining supercurrent (step **II**) outside the absorption area. This increased current density and the local heating lead to the formation of a resistive region across the whole wire (step **III**). The change in impedance for the bias current leads to the creation of a high-frequency pulse used to detect the arrival of single or multiple photons. A typical pulse is shown in the center of Fig. 5.3, with the different detection steps annotated above the pulse. A feedback mechanism between cooling and the inductive response of the superconductor leads to a recovery of the superconductivity (step **IV**) and a recovery of the current density across the wire (step **V**).

While this model allows for a qualitative understanding of the process involved, more sophisticated models have been developed in the last two decades

[178]–[180] to predict beneficial material attributes. A recent Ph.D. Thesis[181] by Jason Allmaras contains a summary of state-of-the-art detection models.

5.3. Measuring Properties of SNSPDs

A typical SNSPD based on NbTiN is biased with a current of approximately $20\mu\text{A}$. The bias and read-out circuit is shown in Figure 5.4a. The current biasing is often realized through a voltage source followed by a high resistance (e.g. $100\text{ k}\Omega$). At the generation of a hotspot, this current is diverted into the high-frequency port of a bias-tee generating a voltage pulse. Either a two-stage amplifier at room-temperature or cryogenic amplification plus room-temperature amplification is necessary to generate a pulse usable for counting a detection event.

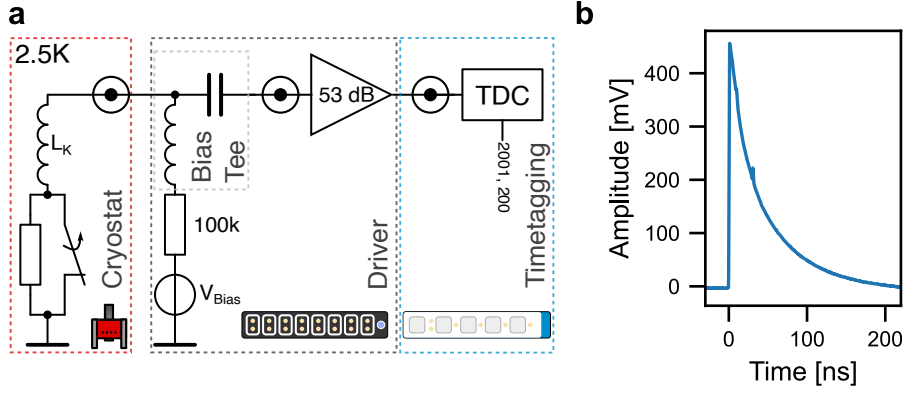


Figure 5.4: **Read-out circuit and detection pulse of an SNSPD.** a) Biasing and read-out circuit of an SNSPD. The SNSPD is modeled as a simple lumped-element circuit. Connected using a coaxial cable is a bias tee that current-biases the SNSPD. The high-frequency path is amplified at room temperature and then connected to either an oscilloscope or a time-to-digital (TDC) converter b) Detection pulse of the SNSPD at the output of the driver, after the room temperature amplifier.

After this amplification, a pulse as shown in Figure 5.4b is measured at the output. In our lab, this amplification and biasing are done using commercial control electronics by Single Quantum (EOS).

Counting these pulses, generated under steady illumination of different wavelengths, and sweeping the bias current allows for measuring the intrinsic detection efficiency of the device (Figure 5.5a). A saturation plateau in the measurement then (like seen in the $\lambda_0 = 850\text{ nm}$ measurement in Figure 5.5a) suggests that all available photons interacting with the nanowire are detected. SNSPDs based on WSi show near internal saturation up to $\lambda_0 = 10\mu\text{m}$ [182],

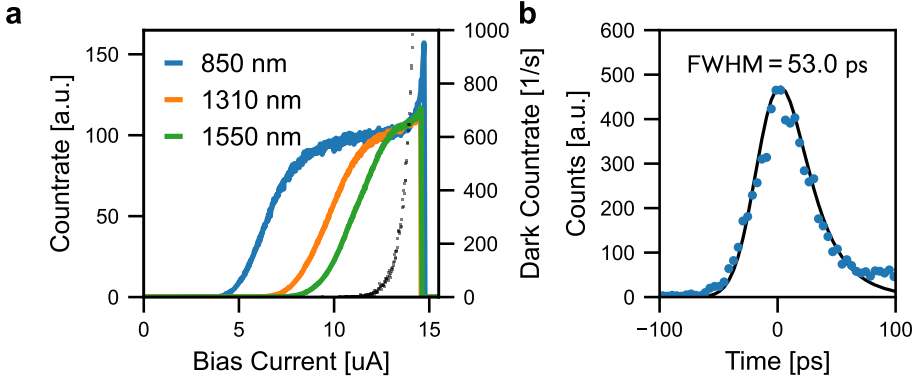


Figure 5.5: **Internal detection efficiency and timing jitter** a) PCR curve of a $16\mu\text{m}$ diameter SNSPD on silicon dioxide for three wavelengths at $\lambda_0 = 850\text{ nm}$, 1310 nm , 1550 nm . Additionally, the dark counts are plotted in grey. b) Detection jitter of $\text{FWHM} = 53.0\text{ ps}$ at $\lambda_0 = 1550\text{ nm}$ employing an impedance matched read-out taper.

while Nb-based detectors have shown saturated detection efficiency at $\lambda_0 = 3\mu\text{m}$ [183].

In comparison, the system detection efficiency is measured by dividing the measured photon flux of the detector by the input power to the fiber leading to the detector. Typical values of more than 80 % are available in commercial detectors but peak detection efficiencies of more than 98 % at 1550 nm have been demonstrated[166].

For time-correlation measurements, the detection events measured by the SNSPDs are then converted into arrival times using a time-to-digital converter (TDC) and written to disk. In our lab, we use a PicoQuant HydraHarp 400 or a quTAG standard as TDC. The files containing the arrival times are evaluated using ETA, a software developed within the research group[184].

A correlation measurement between the laser pulse and the detection pulse is used to characterize the internal device jitter. Thereby the time of generation of the laser pulse signaled by a sync output is compared to the time of detection on an SNSPD. This measurement determines the uncertainty caused by the device and electronics in detection time. The jitter value today for an efficient detector reaches 7.7 ps [185] and $< 3\text{ ps}$ for jitter-optimized structures [165]. Typical commercial SNSPDs have a jitter on the order of 15 ps , which is dependent on the wavelength of the signal. Figure 5.5b shows the shape of this histogram of a large number of detection events, which is typically gaussian or skewed gaussian. Several techniques can be employed to improve the jitter of an SNSPD. By choosing a design with the highest possible critical current for the wavelength of interest, the jitter can be reduced as a higher bias current leads to reduced

jitter. As a second step, cryogenic amplification can be used by operating a wideband RF amplifier inside the cryostat. A different way was suggested by Zhu et al.[186], employing an impedance taper. The RF wave impedance of the nanowires is on the order of a $k\Omega$, if it is directly connected to a 50Ω RF connection, a lot of the energy in the detection pulse is reflected back into the device. A taper structure e.g. a Klopfenstein taper [187], that adiabatically converts from the high impedance structure to a 50Ω transmission line can be used to minimize these reflections. The device shown in Figure 5.5b is based on such an impedance-matched taper.

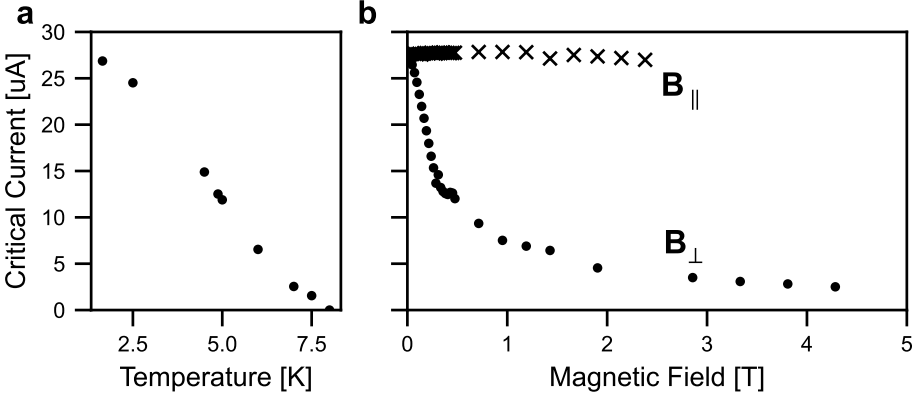


Figure 5.6: **Critical current dependence** for a fiber-coupled SNSPD based on NbTiN. a) Dependence of the critical current on the operating temperature. b) Dependence of the critical current on the magnetic field and its orientation. (B_{\perp} for vertical to the film and B_{\parallel} for parallel to the film.)

Temperature and magnetic field influence the properties of the detector since the detecting concept is based on the superconductive state of a film. Figure 5.6 shows measurements conducted on a fiber-coupled detector based on a 10 nm thick NbTiN film. Figure 5.6a shows the reduction of critical current with increasing temperature. While the optimum detection properties are available at temperatures < 2.5 K, reasonable performance has been demonstrated up to 7 K[188]. In comparison SNSPDs based on amorphous films, like WSi or MoSi, are usually operated at temperatures below 1 K.

Figure 5.6b shows the influence of magnetic fields on SNSPDs. If the plane of the detector is positioned normal to the plane of a magnetic field, it is instantly impacted and can only perform satisfactorily below ≈ 100 mT. In contrast, by turning the SNSPD parallel to the magnetic field (see also Polakovic et al.[189]), greater magnetic field tolerance above 2.5 T can be achieved, allowing single-photon detectors to be installed in high-magnetic field situations. This characteristic, as SNSPDs can detect more than just light, could be a unique selling point in future physics investigations[190].

5.4. Multiplexing and Scale-Up of SNSPDs

A million-pixel SNSPD camera or mm^2 -large area has the potential to be a game-changer. Astronomical imaging at long wavelengths [191], correlation spectroscopy, and depth of field information for each pixel in a photo are just a few examples.

Several factors, such as read-out electronics, fabrication yield, and processing of the vast amount of produced data, impede the development of such a system. We highlight the obstacles for large-scale SNSPD systems beyond the state-of-the-art in **Paper 9**.

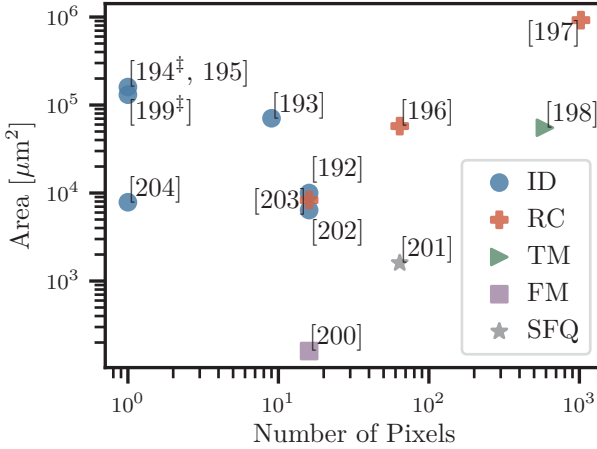


Figure 5.7: **Large-scale SNSPD device comparison.** The area and number of pixels of previously demonstrated devices are compared. [‡] is used to identify microwire-based devices. The devices are categorized by their read-out scheme: individual device readout (ID), row-column readout (RC), time multiplexing (TM), frequency multiplexing (FM), and SFQ-based logic (SFQ). Adapted with permission [205]. (Paper 9)

Scaling up the individual area of a single pixel is limited by the material deposition, the reliability of the nano-fabrication process, and the physical properties of such a device. The film deposition is most commonly based on magnetron sputtering. Other technologies such as plasma-enhanced atomic layer deposition[206] or epitaxial growth[207] promise very uniform film properties. Amorphous materials currently lead the largest patterned SNSPD areas [197], due to more forgiving films concerning substrate non-uniformities and lower patterning demands due to larger structure sizes.

The patterning area is also limited by lithographic methods. Common e-beam write fields are $500\ \mu\text{m}$ or $1000\ \mu\text{m}$. The stitching errors between fields make scaling beyond one write field challenging. The largest single-pixel SNSPDs

currently reported are $400 \times 400 \mu\text{m}^2$ [194], with saturated intrinsic detection efficiency at 1550 nm. Increasing the single-pixel device area increases kinetic inductance and with it increases reset times, additionally the geometric jitter increases[208]. To address the former issue, novel device structures such as parallel nanowires, often known as SNAPs[209], or dividing the device into several pixels are required. The latter can be compensated by using a dual-sided read-out [210].

Additional electronic circuitry enhancements are required to read out many pixels. Several concepts are presented in the following paragraphs.

Individual Device (ID) read-out is the brute-force method of SNSPD scaling and the standard method for single-pixel SNSPDs. An individual coaxial cable is provided for each pixel plus an individual bias-tee, amplifier, and TDC channel are needed. This approach grants high flexibility but creates a substantial heat-load to the cryostat and requires high financial investment. The method allows for providing the lowest jitter and "almost" cross-talk-free operation between pixels.

Row-Column (RC) read-out is the most successful scaling method to date. The pixel number grows with the product of the row and columns, while the coax lines only grow with the sum of those. This allowed recent demonstrations with up to 1024 pixels [197]. While the scaling properties are favorable, the disadvantages are increased cross-talk between devices, the blinding of the whole column and row on detection, and increased jitter. Thermally coupled row-column schemes [203] promise to alleviate some of these disadvantages as the current paths of rows and columns are no longer electrically linked.

Time-multiplexed (TM) read-out depends on correlating the arrival time of the pulse with the source of the detection event through a one-sided or a both-sided readout[211]. Only one or two coaxial lines are needed. To allow for more pixels and clear separation, the propagation properties of the electrical pulse are engineered. Demonstrations of imaging schemes allowed ≈ 590 pixels, with the limitation of a single detection event at a time[198]. Elshaari et al.[212] demonstrates a proof of principle device with two pixels and planar engineered transmission line during this thesis.

Frequency-multiplexed (FM) read-out allows for the scaling of pixels through one coaxial cable. Each pixel is connected to a resonator with an individual resonance frequency[200]. On detection, a ring-down signal generated by the resonator allows identifying the detector.

SFQ logic-based read-out schemes identify the detecting SNSPD using a digital logic family based on superconducting electronics[213]. Single flux quantum (SFQ) logic circuits are based on Josephson junctions as switches. On a detection event, the fast-rising edge is directly sent to the detection logic, while an SFQ circuit generates a serial signal identifying the firing detector.

5.5. Waveguide-Integrated SNSPDs

While planar, meandering SNSPDs represent the current state of the art in low dark counts and high system detection efficiency, SNSPDs integrated on photonic chips (Figure 5.1b) achieved on-chip detection efficiency up to 91 % in 2011[170]. The devices are hairpin-formed nano-wires that are fabricated on top of a waveguide and evanescently coupled to propagating light. The benefit of such an SNSPD is that it can be very broadband[214], can have extremely fast reset times[215], and can be integrated on many material platforms[216] such as Si, SiO₂, GaAs, LiNbO₃. The external system detection efficiency is limited by the coupling to the chip from a fiber, that has to operate at cryogenic temperatures.

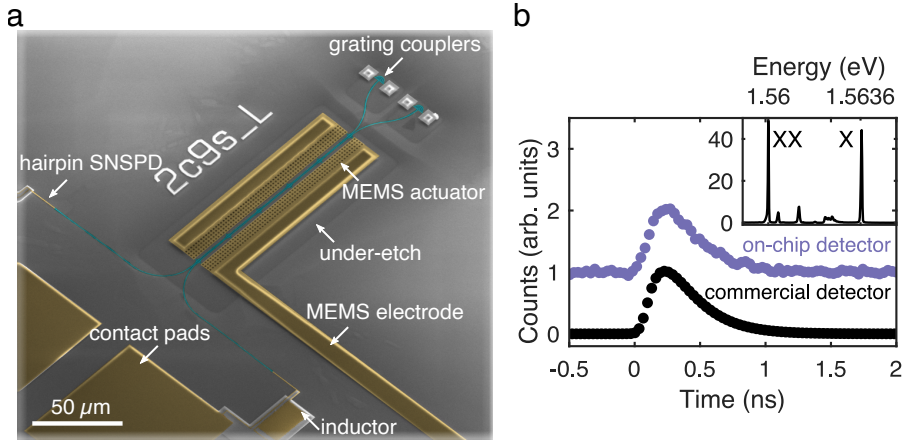


Figure 5.8: **SNSPD co-integrated with reconfigurable photonic circuits.** a) Colored SEM image of the demonstrator device combining SNSPDs and MEMS-based reconfigurable photonics. The individual elements are marked in the picture. b) Lifetime measurement of a quantum dot device emitting at 795 nm. Inset shows the photoluminescence spectra of the exciton (X) and the biexciton (XX). Adapted from [68] (CC BY 4.0) (Paper 1)

During this thesis, we developed the first co-integration of SNSPDs with reconfigurable photonics (See also section 2.4). An SEM scan of the demonstrator device is seen in Figure 5.8a. Commonly reconfigurability is achieved using thermal tuning with typical heater powers of > 10 mW, which is not compatible with the cryogenic operation of SNSPDs[34]. We realize a tunable directional coupler based on MEMS photonics and co-integrated SNSPDs in the process (see also section 2.4 and Paper 1). We demonstrate the compatibility of superconducting nanowire single photon detectors (SNSPD) with the fabrication process of the MEMS circuits including the release step. The chip

consists of a silicon nitride photonic circuit on top of a silicon dioxide BOX layer supported by a silicon substrate. The SNSPDs are patterned and etched first and followed by waveguides that are created using dry etching. As the last step, the SiO_2 below the coupler regions is removed using a buffered hydrofluoric acid (BHF) wet release. This demonstration was possible due to the chemical stable NbTiN film used for the SNSPDs[30]. We use the device to route single photons generated by a quantum dot (see also section 3.7) to a single detector on-chip and measure the lifetime of the transition (Figure 5.8b). We compare the result ($\tau_X = 232$ ps) with a measurement using commercial detectors ($\tau_X = 216$ ps).

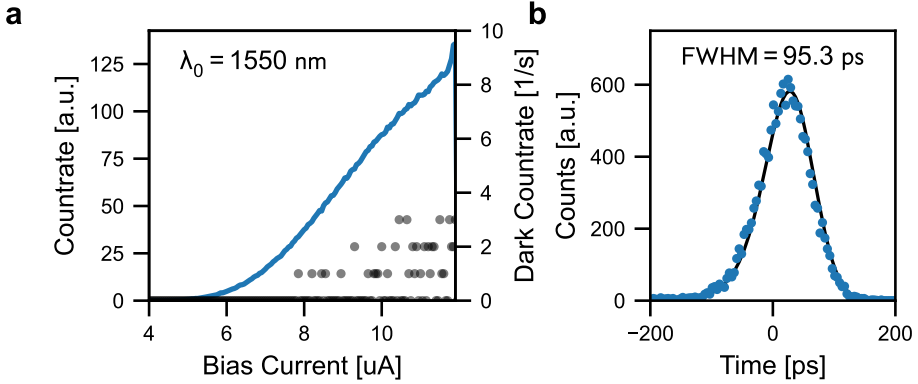


Figure 5.9: **Photon count rate (PCR) and Jitter of SNSPDs on LNOI waveguides.** a) The PCR measurement at 1550 nm of SNSPDs integrated on LNOI rib waveguides. The dark count rate (DCR) is plotted on the right axis. b) Jitter measurement of FWHM = 95.3 ps jitter at $\lambda_0 = 1550$ nm through the LNOI waveguide.

Another way of cryo-compatible reconfiguration is by using an electro-optic material as the guiding layer. Lithium niobate is a promising material due to its maturity developed over decades (see also section 2.2). Implementing SNSPDs is required for future quantum optics experiments such as linear quantum computing, transduction, or feedback control. We presented early results on the integration of SNSPDs on a LiNbO_3 -on-Insulator (LNOI) platform in [65]. To date, several groups have demonstrated integrated SNSPDs on LNOI waveguides with on-chip detection efficiency up to 50 % [217] and in combination with electrooptic modulators [218].

Figure 5.9a shows the photo count rate curve of SNSPDs integrated on LNOI waveguides at 1550 nm, demonstrating close to saturated internal detection efficiency. The system uses free-space coupled grating couplers in a dilution refrigerator with low coupling efficiency limiting the system detection efficiency. The devices showed a jitter of 95.3 ps shown in Figure 5.9b measured through the waveguide.

Waveguide integrated SNSPDs promise to be the detectors for photonic quantum computing, as the optical signal never has to leave the chip. Several businesses, including PsiQuantum, pursue this direction. Once light can be coupled to the chip with high efficiency, building fiber-coupled detectors that are effectively on-chip will make scaling and broad-band operation possible[214].

Conclusions and Outlook

This thesis compiles the outcomes of my Ph.D. work in partnership with the group. It consists of multiple research projects from single photon emitters to single photon detectors coupled to integrated photonic platforms.

Single photon emitters are relevant for future quantum communication networks and photonic quantum computing. We investigated several solid-state emitter candidates, in semiconductors and insulators in the form of defects in MoS_2 and hBN, and quantum dots in InGaAs with spectroscopic and time-correlation measurements.

The emitters in MoS_2 and hBN are good candidates for integration in existing photonic circuits. They emit in the range of 600 nm to 720 nm and are therefore compatible with low-loss silicon nitride photonics. The deterministic integration of hBN single-photon emitters (Paper 4) can allow to match compatible emitters on a chip to achieve photon indistinguishability. Their clean emission lines make filtering for advanced applications easier. A high brightness indicates an efficient emission process.

While the hBN emitter position is post-selected, helium-ion irradiated emitters in MoS_2 can be created after the material stack hBN/ MoS_2 /hBN has been transferred to the photonic platform at an arbitrary position and possibly at a large scale. They can be created with a yield of 18 % at a determined position and emit spectrally clean single photons (Paper 5). An open question for any emitter hosted in 2D materials is if their emitted photons are indistinguishable. Till today, there are no demonstrations of indistinguishable single photon emitters within 2D materials.

Quantum dots on the other hand are emitters with ultra-pure, highly identical, and entangled photon emissions. In our work we utilize quantum dots emitting in the telecom C-band and explored their suitability for future quantum technologies in fiber networks. On emission of entangled photons, those can be degraded by the fine structure splitting. It distinguishes photons from different emitters and requires sub-nanosecond time resolution measurements for photons from a single emitter. It has been shown that through full strain control using a micro-machined piezo actuator the fine structure splitting can be removed[153]. Full strain control on the telecom quantum dots allows tuning

of the FSS from $(12.9 \pm 0.1) \mu\text{eV}$ to $(1.1 \pm 0.1) \mu\text{eV}$ (Paper 7). The generated entangled photons show a maximal fidelity of $(90.0 \pm 2.7) \%$.

By integrating new materials on established photonic platforms, new functionality can be enabled. Cu_2O , a prototype semiconductor, hosts highly excited excitons that lead to strong optical non-linearities and provide a platform for solid-state Rydberg physics. Laboratory growth of micro-crystals allows the integration on silicon platforms (Paper 2), providing a path forward for harnessing its potential.

Another material is WS_2 which can be used to enhance non-linear processes within photonic integrated circuits. By integrating it on silicon nitride (Paper 3), a broadening by almost 50 % in the generated supercontinuum spectra can be achieved.

For many of the mentioned experiments, single photon detection is essential. An excellent technology available today is superconducting nanowire single photon detectors (SNSPDs). They offer high time resolution, high signal-to-noise ratio, and high detection efficiency at wavelengths from UV to the mid-infrared. SNSPDs can be integrated into photonic circuits to allow for on-chip single photon detection. Reconfigurable circuits are often based on heating elements, that make their use with SNSPDs hard to realize. Combining SNSPDs with micro-electromechanical (MEMS) photonics (Paper 1) allows reconfigurability of the photonic circuit and single-photon detection on the same chip. This is a key requirement for future photonic quantum computing or memory nodes in a future quantum network. Our design allows for the routing of single photons with 28 dB extinction and features a photon detector with a 90 dB dynamic range based on the combination of multiple SNSPDs. This combination of technologies is based on a NbTiN[30] film that allows SNSPDs to be developed on multiple substrates (Paper 8) including Si, SiO_2 , LiNbO_3 , or AlN.

Two challenges for SNSPDs can be identified (Paper 9). First, the increase of the detection area to couple them to e.g. free-space optical systems such as telescopes. Recent demonstrations of single photon detection in micrometer wide detection wires may provide a solution for increasing the detection area, as lithography constraints on large-scale areas are more easily met. The second challenge is the read-out of more than a couple of single devices due to the additional challenges created by the heat load of wiring and read-out electronics. Several solutions have been demonstrated for read-out of multiple devices with a row-column read-out and digital labeling of detection pulses using superconducting logic being the most promising for scaling the numbers of pixels.

Where to go from here?

Today, integrated photonics for traditional applications is a multibillion-dollar industry. Two significant applications are transceivers for optical communication as well as light detection and ranging (LIDAR) devices. Although photonics for

quantum technology is still in its infancy in terms of commercial applications, it has been the subject of extensive research over the last decades. Investments in classical photonics are likely to accelerate the exploration of quantum-based applications such as quantum computing and sensing.

Single-photon sources must be further developed for these applications. While excellent values have been achieved for figures of merit such as indistinguishability, single-photon purity, and brightness, many experiments require a combination of multiple properties.

Emitters in 2D materials are in that respect still in an early development stage and the demonstration of indistinguishability of photons emitted by the same source is a requirement for future use as a light source. As they are always close to a material interface, external influences need to be dealt with. One way is through coupling to a high-Q cavity on a photonic chip, which enhances emission into the cavity mode. The helium ion beam-based fabrication would be ideal to realize such a structure.

Quantum dots on the other hand to date are a promising technology to provide quantum light sources. Several future experiments and directions can be envisioned for the telecom quantum dots used in our groups. A big challenge for these dots is the low brightness; the integration of structures enhancing those should be one of the next avenues ahead. Integrating them into diode structures would help in controlling the charge state, probably improving the temporal emission stability. Further investigations into reducing the intrinsic fine-structure and the spread of the created quantum dots could bring them closer to a market-ready product. Their hybrid integration on photonic circuits can be achieved through transfer printing of pre-selected emitters.

The enhancement of existing photonic platforms through hybrid integration holds a big parameter space to explore. Nonlinear properties enhanced through the integration of 2D materials (especially transition metal dichalcogenides, due to the low optical absorption) can then be used for photon-pair generation. The efficient large-scale transfer or growth of optically pure material is a challenge for the field.

The growth of cuprous oxide microcrystals on integrated waveguides allows coupling to integrated resonating structures to utilize the optical non-linearity within the material or the blockade of Rydberg excitons to generate single photons. RF fields interacting with excited Rydberg excitons could allow coherent interaction between optical and microwave fields.

I see the future direction of SNSPDs as measurement tool for experiments within quantum communication, and quantum computing but also photon starved applications like LIDAR, gas sensing, or biological research and diagnostics. To support these applications SNSPDs need to detect further in the mid-infrared while maintaining their excellent properties of high detection efficiency and ideally low dark counts.

Building detection arrays of SNSPDs could create new applications such as time-of-flight imaging with ultra high resolution e.g. to image through scattering

media. Utilizing such an array within a spectrometer would allow for single photon sensitivity, time correlations between spectral features, and a large wavelength range.

SNSPDs integrated into photonic circuits can be utilized for feedback and feed-forward control, where a quantum state is controlled after measurement for quantum computing[219]. Additionally, this could be utilized for complex state preparation or to realize entanglement swapping in a quantum repeater node. The integration as part of foundry processes will give access to lower-budget SNSPDs for a large range of applications.

At last, there are always open questions. Can high-TC superconductors be used for SNSPDs? Where is the limit in time resolution? Can dark matter be found or excluded using SNSPDS?

During my Ph.D., the field of quantum technologies gained momentum/hype, owing to investors and decision makers who do not have the full picture, but also because it promises to solve the hardly solvable and measure the hardly measurable. Even if the end goal will not be reached and promises broken, I believe that funding research into solid physics and hardware is worthwhile for the gold nuggets dropped along the way.

Acknowledgments

Embarking on a big project in life such as getting a Ph.D. is only possible with the support of many people, long before starting the Ph.D. **You are known.**

I would like to thank Prof. Val Zwiller, who got me to Stockholm into the Quantum Nano Photonics group. I am grateful for the freedom I got to invest the money you acquired into a broad collection of projects. It allowed me to work on so many setups, buy so much equipment and access the Nanolab, not to talk about all the conferences I was allowed to visit. I am grateful for that and I am looking forward to further collaborations in the future.

Thank you to Stephan for being a friend and a co-supervisor on this project. I did learn and profit a lot from you, especially in the clean-room, but more will I remember the great atmosphere and hours we spent in and outside work. I appreciate your dedication to getting the science right and the process stable. I hope we will spend more time in the future. Ali, now professor, thank you for being a friend and co-supervisor. Thank you for the trust you placed in me and for teaching me so many things about photonics, quantum optics, and how to achieve 80 % of the result with 20 % of the work. I am very happy for the time our paths ran in parallel and that also part of your dreams got fulfilled. Marijn, thank you for the time you spent in Stockholm and for supporting me on the way to becoming a Ph.D. Klaus, now Professor, left Stockholm before me, but I enjoyed the time we spent on playing board games and on life with you and your family. Thank you for being a friend outside of the lab. I learned so many things from you, from optics in the lab to navigating the scientific process. Thank you for your trust, our paths will cross hopefully many times in the future.

I think I had the best group of Ph.D. students one could have. I am so happy that it was our constellation of people. It was the help in the lab, but also the friendship. We had fun, enjoyed each other's company, and became friends. I hope that these friendships will last into the future. Lucas, your positivity, kindness, and friendliness are extraordinary. I learned so many things from you in the lab, on the computer, and loved tinkering on side projects. Julien, you felt like the most professional of us. Thanks for the time you shared in my Ph.D. journey and your work that made my work possible. Thank you for all the invitations to food and friendship events, that enriched my life outside

the lab. Katha, your determination to make hard things possible, to always stay solution-driven, and to just be a great person to be around. Thank you. Thomas, we stayed the longest in Roslagstull of our Ph.D. circle, and it was good to have you around. It was invaluable support. Your dry humor, your investment in solving a problem carefully, and your critical judgment on my many "ideas" was very appreciated. See you in Austria. Eva, thanks for the time you spent with us. You were completing our team, with your optic knowledge, life energy, and motivation for the sport (which did not infect me though). To the new PhDs, Theodor, Govind, and Morteza, we only had a short time in the same group, but I wish you all the best and take good care of our lab.

Carlos thank you for the collaborations we had in Stockholm and afterward. It was so a lot of fun working with you in the US and spending time in and outside the lab. Thank you to all the people that made up the Quantum Nano Photonics group, especially Lily, Mikael, and Art. You were part of my journey, thanks. Thank you to all the KEX and master students I was fortunate enough to supervise or work with. Selim, Zuzeng, Sandra, Anas, Efe, Josip, Martin, Sven, Ludvig, Erik, Nicolas, Liselott, and James. Part of my work is built on your shoulders and I am grateful for the time you invested into that. Thank you to Prof. Ilja Sytjugov for reviewing my thesis.

Thank you to the staff in the Nanolab; Adrian, Anders, Taras, and Erik, that tried to accommodate my many wishes and improvement ideas. It is a great place to work at. Thank you for all the support I got from the AlbaNova staff, Hugo Svanborg, Mats Sundberg, and the Godsmottagning team, and from the workshop, especially Rolf Helg. Thank you to the staff at Applied Physics for their efforts to accommodate our requests and make the admin experience more enjoyable.

Thank you to Alessandro and Amin, you were our A-team providing excellent LNOI products, but also a lot of joy, laughter, and knowledge. It always made my day seeing one of you around AlbaNova. Thank you to Mattias, Robert, Jack and Mats, Gunnar, and Marcin for discussing SNSPDs again and again with us, working on models and measurements on our devices. Antonio, it was great to have you in Stockholm several times and spent time in the lab figuring out FPGAs and modulators. Jin, Iman, and Andreas, thank you for the work you did in Delft for us and the support we got from you.

Thank you to all the collaborators I was fortunate enough to work with. Oskars, thank you for your support on anything RF and for providing your equipment. Katja, Julian, Xandy, and Alex, it was great to use your nicely placed emitters, and spend some lab time in Stockholm with you. Yuchen and Prof. Sun, thank you for making use of my waveguides. Prof. Hu and your team, it is great to see you make such nice devices with our superconducting films. Thanks to you, Mariia and Alexej, we know our films much better now. Valeria, Mihika, Connor, Chris, and Dirk, it was great to measure in your lab, I enjoyed the time I stayed with you. Thank you to the quantum dot growers, who manufactured the samples I used for my results. The team at KTH with

Mattias Hammar and Carl Reuterskiöld Hedlund, the team in Linz of Armando Rastelli, and the team of Dan Dalacu and Philip J. Poole.

I would like to thank my parents and family who supported me in following my dreams and my curiosity through their emotional and financial support. All my friends from Schladming, Zürich and Stockholm, thanks for being there. Thank you to Yvonne, the partner on my side for project Ph.D., and Project Life. It is so good to have your support, motivation, and joy. You complement me, thank you.

For all the time, love, and energy invested in me, I will pay it forward.

Bibliography

- [1] M. D. Al-Amri, M. El-Gomati, and M. S. Zubairy, Eds., *Optics in Our Time*. Cham: Springer International Publishing, 2016.
- [2] P. A. M. Dirac, “The quantum theory of the emission and absorption of radiation,” *Proceedings of the Royal Society of London. Series A, Containing Papers of a Mathematical and Physical Character*, vol. 114, no. 767, pp. 243–265, Mar. 1927.
- [3] R. J. Glauber, “The Quantum Theory of Optical Coherence,” *Physical Review*, vol. 130, no. 6, pp. 2529–2539, Jun. 1963.
- [4] R. J. Glauber, “Coherent and Incoherent States of the Radiation Field,” *Physical Review*, vol. 131, no. 6, pp. 2766–2788, Sep. 1963.
- [5] A. G. J. MacFarlane, J. P. Dowling, and G. J. Milburn, “Quantum technology: The second quantum revolution,” *Philosophical Transactions of the Royal Society of London. Series A: Mathematical, Physical and Engineering Sciences*, vol. 361, no. 1809, pp. 1655–1674, Aug. 2003.
- [6] R. H. Brown and R. Q. Twiss, “Correlation between Photons in two Coherent Beams of Light,” *Nature*, vol. 177, no. 4497, pp. 27–29, Jan. 1956.
- [7] H. J. Kimble, M. Dagenais, and L. Mandel, “Photon Antibunching in Resonance Fluorescence,” *Physical Review Letters*, vol. 39, no. 11, pp. 691–695, Sep. 1977.
- [8] R. E. Slusher, L. W. Hollberg, B. Yurke, J. C. Mertz, and J. F. Valley, “Observation of Squeezed States Generated by Four-Wave Mixing in an Optical Cavity,” *Physical Review Letters*, vol. 55, no. 22, pp. 2409–2412, Nov. 1985.
- [9] C. K. Hong, Z. Y. Ou, and L. Mandel, “Measurement of subpicosecond time intervals between two photons by interference,” *Physical Review Letters*, vol. 59, no. 18, pp. 2044–2046, Nov. 1987.
- [10] Z. Ahmed, Y. Alexeev, G. Apollinari, *et al.*, “Quantum Sensing for High Energy Physics,” *arXiv:1803.11306 [hep-ex, physics:hep-ph, physics:physics]*, Mar. 2018.
- [11] B. J. Lawrie, P. D. Lett, A. M. Marino, and R. C. Pooser, “Quantum Sensing with Squeezed Light,” *ACS Photonics*, vol. 6, no. 6, pp. 1307–1318, Jun. 2019.

- [12] J. Aasi, J. Abadie, B. P. Abbott, *et al.*, “Enhanced sensitivity of the LIGO gravitational wave detector by using squeezed states of light,” *Nature Photonics*, vol. 7, no. 8, pp. 613–619, Aug. 2013.
- [13] R. P. Feynman, “Simulating physics with computers,” *International Journal of Theoretical Physics*, vol. 21, no. 6, pp. 467–488, Jun. 1982.
- [14] F. Arute, K. Arya, R. Babbush, *et al.*, “Quantum supremacy using a programmable superconducting processor,” *Nature*, vol. 574, no. 7779, pp. 505–510, Oct. 2019.
- [15] T. D. Ladd, F. Jelezko, R. Laflamme, Y. Nakamura, C. Monroe, and J. L. O’Brien, “Quantum computers,” *Nature*, vol. 464, no. 7285, pp. 45–53, Mar. 2010.
- [16] C. H. Bennett and G. Brassard, “Quantum Cryptography: Public Key Distribution and Coin Tossing,” in *Proceedings of IEEE International Conference on Computers, Systems and Signal Processing*, Bangalore, Dec. 1984, pp. 175–179.
- [17] A. K. Ekert, “Quantum cryptography based on Bell’s theorem,” *Physical Review Letters*, vol. 67, no. 6, pp. 661–663, Aug. 1991.
- [18] S. Wehner, D. Elkouss, and R. Hanson, “Quantum internet: A vision for the road ahead,” *Science*, vol. 362, no. 6412, eaam9288, Oct. 2018.
- [19] D. Gottesman, T. Jennewein, and S. Croke, “Longer-Baseline Telescopes Using Quantum Repeaters,” *Physical Review Letters*, vol. 109, no. 7, p. 070 503, Aug. 2012.
- [20] R. Soref and B. Bennett, “Electrooptical effects in silicon,” *IEEE Journal of Quantum Electronics*, vol. 23, no. 1, pp. 123–129, Jan. 1987.
- [21] Q. Cheng, M. Bahadori, M. Glick, S. Rumley, and K. Bergman, “Recent advances in optical technologies for data centers: A review,” *Optica*, vol. 5, no. 11, pp. 1354–1370, Nov. 2018.
- [22] YOLE Développement, *Si photonics: Beyond the tipping point*, May 2019.
- [23] S. Y. Siew, B. Li, F. Gao, *et al.*, “Review of Silicon Photonics Technology and Platform Development,” *Journal of Lightwave Technology*, vol. 39, no. 13, pp. 4374–4389, Jul. 2021.
- [24] D. J. Blumenthal, R. Heideman, D. Geuzebroek, A. Leinse, and C. Roeloffzen, “Silicon Nitride in Silicon Photonics,” *Proceedings of the IEEE*, vol. 106, no. 12, pp. 2209–2231, Dec. 2018.
- [25] A. Politi, J. C. Matthews, M. G. Thompson, and J. L. O’Brien, “Integrated Quantum Photonics,” *IEEE Journal of Selected Topics in Quantum Electronics*, vol. 15, no. 6, pp. 1673–1684, Nov. 2009.
- [26] T. Honjo, K. Inoue, and H. Takahashi, “Differential-phase-shift quantum key distribution experiment with a planar light-wave circuit Mach–Zehnder interferometer,” *Optics Letters*, vol. 29, no. 23, pp. 2797–2799, Dec. 2004.
- [27] J. Wang, F. Sciarrino, A. Laing, and M. G. Thompson, “Integrated photonic quantum technologies,” *Nature Photonics*, vol. 14, no. 5, pp. 273–284, May 2020.

- [28] G. Moody, V. Sorger, P. Juodawlkis, *et al.*, “Roadmap on integrated quantum photonics,” *Journal of Physics: Photonics*, 2021.
- [29] J. Klein, M. Lorke, M. Florian, *et al.*, “Site-selectively generated photon emitters in monolayer MoS₂ via local helium ion irradiation,” *Nature Communications*, vol. 10, no. 1, pp. 1–8, Jun. 2019.
- [30] J. Zichi, J. Chang, S. Steinhauer, *et al.*, “Optimizing the stoichiometry of ultrathin NbTiN films for high-performance superconducting nanowire single-photon detectors,” *Optics Express*, vol. 27, no. 19, pp. 26 579–26 587, Sep. 2019.
- [31] Omdia, “Global Fiber Development Index: 2020,” Omdia, White Paper, 2020.
- [32] Corning, “Corning SMF-28 Optical Fiber,” Corning, New York, Datasheet PI1036, Apr. 2002.
- [33] R. V. Schmidt and I. P. Kaminow, “Metal-diffused optical waveguides in LiNbO₃,” *Applied Physics Letters*, vol. 25, no. 8, pp. 458–460, Oct. 1974.
- [34] L. Chrostowski and M. Hochberg, *Silicon Photonics Design*. Cambridge: Cambridge University Press, 2015.
- [35] Hammer, M, *Mode solver for 2-D multilayer waveguides*, <https://www.sioo.eu/eims.html>.
- [36] C. Scarcella, J. S. Lee, C. Eason, *et al.*, “PLAT4M: Progressing Silicon Photonics in Europe,” *Photonics*, vol. 3, no. 1, p. 1, Mar. 2016.
- [37] J. F. Bauters, M. J. R. Heck, D. D. John, *et al.*, “Planar waveguides with less than 0.1 dB/m propagation loss fabricated with wafer bonding,” *Optics Express*, vol. 19, no. 24, pp. 24 090–24 101, Nov. 2011.
- [38] J. Liu, G. Huang, R. N. Wang, *et al.*, “High-yield, wafer-scale fabrication of ultralow-loss, dispersion-engineered silicon nitride photonic circuits,” *Nature Communications*, vol. 12, no. 1, p. 2236, Apr. 2021.
- [39] X. Ji, F. A. S. Barbosa, S. P. Roberts, *et al.*, “Ultra-low-loss on-chip resonators with sub-milliwatt parametric oscillation threshold,” *Optica*, vol. 4, no. 6, p. 619, Jun. 2017.
- [40] D. B. Davidson, *Computational Electromagnetics for RF and Microwave Engineering*. Leiden: Cambridge University Press, 2005.
- [41] A. Taflov, “Application of the Finite-Difference Time-Domain Method to Sinusoidal Steady-State Electromagnetic-Penetration Problems,” *IEEE Transactions on Electromagnetic Compatibility*, vol. EMC-22, no. 3, pp. 191–202, Aug. 1980.
- [42] K. Yee, “Numerical solution of initial boundary value problems involving maxwell’s equations in isotropic media,” *IEEE Transactions on Antennas and Propagation*, vol. 14, no. 3, pp. 302–307, May 1966.
- [43] M. Smit, K. Williams, and J. van der Tol, “Past, present, and future of InP-based photonic integration,” *APL Photonics*, vol. 4, no. 5, p. 050 901, May 2019.
- [44] L. Chang, G. D. Cole, G. Moody, and J. E. Bowers, “CSOI: Beyond Silicon-on-Insulator Photonics,” *Optics and Photonics News*, vol. 33, no. 1, p. 24, Jan. 2022.

- [45] Y. Wang, K. D. Jöns, and Z. Sun, “Integrated photon-pair sources with nonlinear optics,” *Applied Physics Reviews*, vol. 8, no. 1, p. 011 314, Mar. 2021.
- [46] M. D. Dvorak and B. L. Justus, “Z-scan studies of nonlinear absorption and refraction in bulk, undoped InP,” *Optics Communications*, vol. 114, no. 1, pp. 147–150, Jan. 1995.
- [47] R. L. Sutherland, D. G. McLean, and S. Kirkpatrick, *Handbook of Nonlinear Optics* (Optical Engineering 82), 2nd ed., rev. and expanded. New York: Marcel Dekker, 2003.
- [48] M. W. Puckett, K. Liu, N. Chauhan, *et al.*, “422 Million intrinsic quality factor planar integrated all-waveguide resonator with sub-MHz linewidth,” *Nature Communications*, vol. 12, no. 1, p. 934, Feb. 2021.
- [49] M. Zhang, C. Wang, R. Cheng, A. Shams-Ansari, and M. Lončar, “Monolithic ultra-high-Q lithium niobate microring resonator,” *Optica*, vol. 4, no. 12, pp. 1536–1537, Dec. 2017.
- [50] W. H. P. Pernice, C. Xiong, C. Schuck, and H. X. Tang, “Second harmonic generation in phase matched aluminum nitride waveguides and microring resonators,” *Applied Physics Letters*, vol. 100, no. 22, p. 223 501, May 2012.
- [51] M. Pu, L. Ottaviano, E. Semenova, and K. Yvind, “Efficient frequency comb generation in AlGaAs-on-insulator,” *Optica*, vol. 3, no. 8, pp. 823–826, Aug. 2016.
- [52] M. A. Guidry, K. Y. Yang, D. M. Lukin, *et al.*, “Optical parametric oscillation in silicon carbide nanophotonics,” *Optica*, vol. 7, no. 9, pp. 1139–1142, Sep. 2020.
- [53] H. Sato, M. Abe, I. Shoji, J. Suda, and T. Kondo, “Accurate measurements of second-order nonlinear optical coefficients of 6H and 4H silicon carbide,” *JOSA B*, vol. 26, no. 10, pp. 1892–1896, Oct. 2009.
- [54] X. Guo, Z. Peng, P. Ding, *et al.*, “Nonlinear optical properties of 6H-SiC and 4H-SiC in an extensive spectral range,” *Optical Materials Express*, vol. 11, no. 4, pp. 1080–1092, Apr. 2021.
- [55] D. J. Wilson, K. Schneider, S. Hönl, *et al.*, “Integrated gallium phosphide nonlinear photonics,” *Nature Photonics*, vol. 14, no. 1, pp. 57–62, Jan. 2020.
- [56] D. J. Moss, R. Morandotti, A. L. Gaeta, and M. Lipson, “New CMOS-compatible platforms based on silicon nitride and Hydex for nonlinear optics,” *Nature Photonics*, vol. 7, no. 8, pp. 597–607, Aug. 2013.
- [57] C. H. Henry, R. F. Kazarinov, H. J. Lee, K. J. Orlowsky, and L. E. Katz, “Low loss Si_3N_4 - SiO_2 optical waveguides on Si,” *Applied Optics*, vol. 26, no. 13, pp. 2621–2624, Jul. 1987.
- [58] K. Ikeda, R. E. Saperstein, N. Alic, and Y. Fainman, “Thermal and Kerr nonlinear properties of plasma-deposited silicon nitride/silicon dioxide waveguides,” *Optics Express*, vol. 16, no. 17, pp. 12 987–12 994, Aug. 2008.

- [59] H. E. Dirani, L. Youssef, C. Petit-Etienne, *et al.*, “Ultralow-loss tightly confining Si_3N_4 waveguides and high-Q microresonators,” *Optics Express*, vol. 27, no. 21, p. 30 726, Oct. 2019.
- [60] D. Zhu, L. Shao, M. Yu, *et al.*, “Integrated photonics on thin-film lithium niobate,” *Advances in Optics and Photonics*, vol. 13, no. 2, pp. 242–352, Jun. 2021.
- [61] M. Bazzan and C. Sada, “Optical waveguides in lithium niobate: Recent developments and applications,” *Applied Physics Reviews*, vol. 2, no. 4, p. 040 603, Dec. 2015.
- [62] P. R. Sharapova, K. H. Luo, H. Herrmann, M. Reichelt, T. Meier, and C. Silberhorn, “Toolbox for the design of LiNbO_3 -based passive and active integrated quantum circuits,” *New Journal of Physics*, vol. 19, no. 12, p. 123 009, Dec. 2017.
- [63] P. Rabiei and P. Gunter, “Optical and electro-optical properties of submicrometer lithium niobate slab waveguides prepared by crystal ion slicing and wafer bonding,” *Applied Physics Letters*, vol. 85, no. 20, pp. 4603–4605, Nov. 2004.
- [64] H. Hu, R. Ricken, and W. Sohler, “Large area, crystal-bonded LiNbO_3 thin films and ridge waveguides of high refractive index contrast,” in *Photorefractive Materials, Effects, and Devices - Control of Light and Matter*, Bad Honnef, Jun. 2009.
- [65] J. Zichi, S. Gyger, M. A. Baghban, A. W. Elshaari, K. Gallo, and V. Zwiller, “An NbTiN superconducting single photon detector implemented on a LiNbO_3 nano-waveguide at telecom wavelength,” in *ECIO 2019*, 2019.
- [66] X. Zhang, K. Kwon, J. Henriksson, J. Luo, and M. C. Wu, “A large-scale microelectromechanical-systems-based silicon photonics LiDAR,” *Nature*, vol. 603, no. 7900, pp. 253–258, Mar. 2022.
- [67] C. Errando-Herranz, A. Y. Takabayashi, P. Edinger, H. Sattari, K. B. Gylfason, and N. Quack, “MEMS for Photonic Integrated Circuits,” *IEEE Journal of Selected Topics in Quantum Electronics*, vol. 26, no. 2, pp. 1–16, Mar. 2020.
- [68] S. Gyger, J. Zichi, L. Schweickert, *et al.*, “Reconfigurable photonics with on-chip single-photon detectors,” *Nature Communications*, vol. 12, no. 1, p. 1408, Mar. 2021.
- [69] K. Kato and Y. Tohmori, “PLC hybrid integration technology and its application to photonic components,” *IEEE Journal of Selected Topics in Quantum Electronics*, vol. 6, no. 1, pp. 4–13, Jan. 2000.
- [70] B. B. Bakir, A. Descos, N. Olivier, *et al.*, “Electrically driven hybrid $\text{Si}/\text{III-V}$ Fabry-Pérot lasers based on adiabatic mode transformers,” *Optics Express*, vol. 19, no. 11, pp. 10 317–10 325, May 2011.
- [71] C. O. de Beeck, B. Haq, L. Elsinger, *et al.*, “Heterogeneous III-V on silicon nitride amplifiers and lasers via microtransfer printing,” *Optica*, vol. 7, no. 5, pp. 386–393, May 2020.

- [72] C. O. de Beeck, F. M. Mayor, S. Cuyvers, *et al.*, “III/V-on-lithium niobate amplifiers and lasers,” *Optica*, vol. 8, no. 10, pp. 1288–1289, Oct. 2021.
- [73] P. O. Weigel, J. Zhao, K. Fang, *et al.*, “Bonded thin film lithium niobate modulator on a silicon photonics platform exceeding 100 GHz 3-dB electrical modulation bandwidth,” *Optics Express*, vol. 26, no. 18, pp. 23 728–23 739, Sep. 2018.
- [74] N. Boynton, H. Cai, M. Gehl, *et al.*, “A heterogeneously integrated silicon photonic/lithium niobate travelling wave electro-optic modulator,” *Optics Express*, vol. 28, no. 2, pp. 1868–1884, Jan. 2020.
- [75] P. Kaur, A. Boes, G. Ren, T. G. Nguyen, G. Roelkens, and A. Mitchell, “Hybrid and heterogeneous photonic integration,” *APL Photonics*, vol. 6, no. 6, p. 061 102, Jun. 2021.
- [76] W. H. Brattain, “The Copper Oxide Rectifier,” *Reviews of Modern Physics*, vol. 23, no. 3, pp. 203–212, Jul. 1951.
- [77] E. F. Gross, “Optical spectrum of excitons in the crystal lattice,” *Il Nuovo Cimento (1955-1965)*, vol. 3, no. 4, pp. 672–701, Apr. 1956.
- [78] M. Hayashi, “Absorption Spectrum of Cuprous Oxide in the Visible Region,” *Journal of the Faculty of Science, Hokkaido University, Japan*, vol. IV, no. 2, pp. 107–128, 1952.
- [79] S. A. Moskalenko and D. W. Snoke, *Bose-Einstein Condensation of Excitons and Biexcitons: And Coherent Nonlinear Optics with Excitons*, digitally printed first paperback version. Cambridge: Cambridge University Press, 2005.
- [80] L. C. Olsen, F. W. Addis, and W. Miller, “Experimental and theoretical studies of Cu₂O solar cells,” *Solar Cells*, vol. 7, no. 3, pp. 247–279, Dec. 1982.
- [81] S. Shibasaki, Y. Honishi, N. Nakagawa, *et al.*, “Highly transparent Cu₂O absorbing layer for thin film solar cells,” *Applied Physics Letters*, vol. 119, no. 24, p. 242 102, Dec. 2021.
- [82] T. Kazimierczuk, D. Fröhlich, S. Scheel, H. Stolz, and M. Bayer, “Giant Rydberg excitons in the copper oxide Cu₂O,” *Nature*, vol. 514, no. 7522, pp. 343–347, Oct. 2014.
- [83] M. A. M. Versteegh, S. Steinhauer, J. Bajo, *et al.*, “Giant Rydberg excitons in $\{\mathrm{Cu}\}_{-2}\mathrm{O}$ probed by photoluminescence excitation spectroscopy,” *Physical Review B*, vol. 104, no. 24, p. 245 206, Dec. 2021.
- [84] S. Steinhauer, M. A. M. Versteegh, S. Gyger, *et al.*, “Rydberg excitons in Cu₂O microcrystals grown on a silicon platform,” *Communications Materials*, vol. 1, no. 1, pp. 1–7, Mar. 2020.
- [85] S. Mani, J. I. Jang, J. B. Ketterson, and H. Y. Park, “High-quality Cu₂O crystals with various morphologies grown by thermal oxidation,” *Journal of Crystal Growth*, vol. 311, no. 14, pp. 3549–3552, Jul. 2009.

- [86] V. Walthers, R. Johnes, and T. Pohl, "Giant optical nonlinearities from Rydberg excitons in semiconductor microcavities," *Nature Communications*, vol. 9, no. 1, p. 1309, Apr. 2018.
- [87] K. F. Mak and J. Shan, "Photonics and optoelectronics of 2D semiconductor transition metal dichalcogenides," *Nature Photonics*, vol. 10, no. 4, pp. 216–226, Apr. 2016.
- [88] C. Lan, C. Li, J. C. Ho, and Y. Liu, "2D WS₂: From Vapor Phase Synthesis to Device Applications," *Advanced Electronic Materials*, vol. 7, no. 7, p. 2000688, 2021.
- [89] Y. Wang, V. Pelgrin, S. Gyger, *et al.*, "Enhancing Si₃N₄ Waveguide Nonlinearity with Heterogeneous Integration of Few-Layer WS₂," *ACS Photonics*, vol. 8, no. 9, pp. 2713–2721, Sep. 2021.
- [90] S. Castelletto, "Silicon carbide single-photon sources: Challenges and prospects," *Materials for Quantum Technology*, vol. 1, no. 2, p. 023001, Mar. 2021.
- [91] W. Redjem, A. Durand, T. Herzig, *et al.*, "Single artificial atoms in silicon emitting at telecom wavelengths," *Nature Electronics*, vol. 3, no. 12, pp. 738–743, Dec. 2020.
- [92] A. W. Elshaari, W. Pernice, K. Srinivasan, O. Benson, and V. Zwiller, "Hybrid integrated quantum photonic circuits," *Nature Photonics*, pp. 1–14, Apr. 2020.
- [93] C. Errando-Herranz, E. Schöll, R. Picard, *et al.*, "Resonance Fluorescence from Waveguide-Coupled, Strain-Localized, Two-Dimensional Quantum Emitters," *ACS Photonics*, Apr. 2021.
- [94] A. W. Elshaari, E. Büyükozer, I. E. Zadeh, *et al.*, "Strain-Tunable Quantum Integrated Photonics," *Nano Letters*, Nov. 2018.
- [95] N. J. D. Martinez, C. T. Derose, R. W. Brock, *et al.*, "High performance waveguide-coupled Ge-on-Si linear mode avalanche photodiodes," *Optics Express*, vol. 24, no. 17, pp. 19072–19081, Aug. 2016.
- [96] M. Fox, *Quantum Optics: An Introduction* (Oxford Master Series in Physics 15). Oxford ; New York: Oxford University Press, 2006.
- [97] C. C. Gerry and P. Knight, *Introductory Quantum Optics*. Cambridge, UK; New York: Cambridge University Press, 2005.
- [98] W.-Y. Hwang, "Quantum Key Distribution with High Loss: Toward Global Secure Communication," *Physical Review Letters*, vol. 91, no. 5, p. 057901, Aug. 2003.
- [99] H.-K. Lo, X. Ma, and K. Chen, "Decoy State Quantum Key Distribution," *Physical Review Letters*, vol. 94, no. 23, p. 230504, Jun. 2005.
- [100] X. Ma, B. Qi, Y. Zhao, and H.-K. Lo, "Practical decoy state for quantum key distribution," *Physical Review A*, vol. 72, no. 1, p. 012326, Jul. 2005.
- [101] B. Y. Zel'Dovich and D. N. Klyshko, "Field Statistics in Parametric Luminescence," *Soviet Journal of Experimental and Theoretical Physics Letters*, vol. 9, p. 40, Jan. 1969.

- [102] D. C. Burnham and D. L. Weinberg, "Observation of Simultaneity in Parametric Production of Optical Photon Pairs," *Physical Review Letters*, vol. 25, no. 2, pp. 84–87, Jul. 1970.
- [103] P. G. Kwiat, K. Mattle, H. Weinfurter, A. Zeilinger, A. V. Sergienko, and Y. Shih, "New High-Intensity Source of Polarization-Entangled Photon Pairs," *Physical Review Letters*, vol. 75, no. 24, pp. 4337–4341, Dec. 1995.
- [104] E. Meyer-Scott, C. Silberhorn, and A. Migdall, "Single-photon sources: Approaching the ideal through multiplexing," *Review of Scientific Instruments*, vol. 91, no. 4, p. 041 101, Apr. 2020.
- [105] P. Grangier, G. Roger, and A. Aspect, "Experimental Evidence for a Photon Anticorrelation Effect on a Beam Splitter: A New Light on Single-Photon Interferences," *Europhysics Letters (EPL)*, vol. 1, no. 4, pp. 173–179, Feb. 1986.
- [106] B. Hensen, H. Bernien, A. E. Dréau, *et al.*, "Loophole-free Bell inequality violation using electron spins separated by 1.3 kilometres," *Nature*, vol. 526, no. 7575, pp. 682–686, Oct. 2015.
- [107] L. Schweickert, K. D. Jöns, K. D. Zeuner, *et al.*, "On-demand generation of background-free single photons from a solid-state source," *Applied Physics Letters*, vol. 112, no. 9, p. 093 106, Feb. 2018.
- [108] P. Senellart, G. Solomon, and A. White, "High-performance semiconductor quantum-dot single-photon sources," *Nature Nanotechnology*, vol. 12, no. 11, pp. 1026–1039, Nov. 2017.
- [109] P. Michler, Ed., *Quantum Dots for Quantum Information Technologies* (Nano-Optics and Nanophotonics). Cham: Springer International Publishing, 2017.
- [110] K. Takemoto, Y. Nambu, T. Miyazawa, *et al.*, "Quantum key distribution over 120 km using ultrahigh purity single-photon source and superconducting single-photon detectors," *Scientific Reports*, vol. 5, p. 14 383, Sep. 2015.
- [111] A. Orioux, M. A. M. Versteegh, K. D. Jöns, and S. Ducci, "Semiconductor devices for entangled photon pair generation: A review," *Reports on Progress in Physics*, vol. 80, no. 7, p. 076 001, Jul. 2017.
- [112] K. Heshami, D. G. England, P. C. Humphreys, *et al.*, "Quantum memories: Emerging applications and recent advances," *Journal of Modern Optics*, vol. 63, no. 20, pp. 2005–2028, Nov. 2016.
- [113] K. Zeuner, "Semiconductor Quantum Optics at Telecom Wavelengths," Ph.D. dissertation, KTH Royal Institute of Technology, 2020.
- [114] S. Gyger, K. D. Zeuner, K. D. Jöns, *et al.*, "Reconfigurable frequency coding of triggered single photons in the telecom C-band," *Optics Express*, vol. 27, no. 10, p. 14 400, May 2019.
- [115] K. Brunner, G. Abstreiter, G. Böhm, G. Tränkle, and G. Weimann, "Sharp-Line Photoluminescence and Two-Photon Absorption of Zero-Dimensional Biexcitons in a GaAs/AlGaAs Structure," *Physical Review Letters*, vol. 73, no. 8, pp. 1138–1141, Aug. 1994.

- [116] R. J. Young, R. M. Stevenson, A. J. Shields, *et al.*, “Inversion of exciton level splitting in quantum dots,” *Physical Review B*, vol. 72, no. 11, p. 113 305, Sep. 2005.
- [117] G. Baym, “The physics of hanbury brown-twiss intensity interferometry: From stars to nuclear collisions.,” *Acta Physica Polonica. B*, vol. B29, no. 7, pp. 1839–1884, 1998.
- [118] A. W. Elshaari, A. Skalli, S. Gyger, *et al.*, “Deterministic Integration of hBN Emitter in Silicon Nitride Photonic Waveguide,” *Advanced Quantum Technologies*, vol. 4, no. 6, p. 2 100 032, 2021.
- [119] C. Bradac, W. Gao, J. Forneris, M. E. Trusheim, and I. Aharonovich, “Quantum nanophotonics with group IV defects in diamond,” *Nature Communications*, vol. 10, no. 1, p. 5625, Dec. 2019.
- [120] V. A. Norman, S. Majety, Z. Wang, W. H. Casey, N. Curro, and M. Radulaski, “Novel color center platforms enabling fundamental scientific discovery,” *InfoMat*, vol. 3, no. 8, pp. 869–890, 2021.
- [121] S. Castelletto, F. A. Inam, S.-i. Sato, and A. Boretti, “Hexagonal boron nitride: A review of the emerging material platform for single-photon sources and the spin–photon interface,” *Beilstein Journal of Nanotechnology*, vol. 11, no. 1, pp. 740–769, May 2020.
- [122] J. Klein, L. Sigl, S. Gyger, *et al.*, “Engineering the Luminescence and Generation of Individual Defect Emitters in Atomically Thin MoS₂,” *ACS Photonics*, vol. 8, no. 2, pp. 669–677, Feb. 2021.
- [123] S. Manzeli, D. Ovchinnikov, D. Pasquier, O. V. Yazyev, and A. Kis, “2D transition metal dichalcogenides,” *Nature Reviews Materials*, vol. 2, no. 8, pp. 1–15, Jun. 2017.
- [124] X. Liu and M. C. Hersam, “2D materials for quantum information science,” *Nature Reviews Materials*, vol. 4, no. 10, pp. 669–684, Oct. 2019.
- [125] E. Y. Andrei, D. K. Efetov, P. Jarillo-Herrero, *et al.*, “The marvels of moiré materials,” *Nature Reviews Materials*, vol. 6, no. 3, pp. 201–206, Mar. 2021.
- [126] P. Tonndorf, R. Schmidt, R. Schneider, *et al.*, “Single-photon emission from localized excitons in an atomically thin semiconductor,” *Optica*, vol. 2, no. 4, pp. 347–352, Apr. 2015.
- [127] A. Srivastava, M. Sidler, A. V. Allain, D. S. Lembke, A. Kis, and A. Imamoglu, “Optically active quantum dots in monolayer WSe₂,” *Nature Nanotechnology*, vol. 10, no. 6, pp. 491–496, Jun. 2015.
- [128] M. Koperski, K. Nogajewski, A. Arora, *et al.*, “Single photon emitters in exfoliated WSe₂ structures,” *Nature Nanotechnology*, vol. 10, no. 6, pp. 503–506, Jun. 2015.
- [129] Y.-M. He, G. Clark, J. R. Schaibley, *et al.*, “Single quantum emitters in monolayer semiconductors,” *Nature Nanotechnology*, vol. 10, no. 6, pp. 497–502, Jun. 2015.

- [130] S. I. Azzam, K. Parto, and G. Moody, “Prospects and challenges of quantum emitters in 2D materials,” *Applied Physics Letters*, vol. 118, no. 24, p. 240 502, Jun. 2021.
- [131] E. Mitterreiter, B. Schuler, A. Micevic, *et al.*, “The role of chalcogen vacancies for atomic defect emission in MoS₂,” *Nature Communications*, vol. 12, no. 1, p. 3822, Jun. 2021.
- [132] Y. H. Huo, A. Rastelli, and O. G. Schmidt, “Ultra-small excitonic fine structure splitting in highly symmetric quantum dots on GaAs (001) substrate,” *Applied Physics Letters*, vol. 102, no. 15, p. 152 105, Apr. 2013.
- [133] T. Müller, J. Skiba-Szymanska, A. B. Krysa, *et al.*, “A quantum light-emitting diode for the standard telecom window around 1,550 nm,” *Nature Communications*, vol. 9, no. 1, p. 862, Feb. 2018.
- [134] M. Paul, F. Olbrich, J. Höschele, *et al.*, “Single-photon emission at 1.55 μ m from MOVPE-grown InAs quantum dots on InGaAs/GaAs metamorphic buffers,” *Applied Physics Letters*, vol. 111, no. 3, p. 033 102, Jul. 2017.
- [135] P. Michler, A. Kiraz, C. Becher, *et al.*, “A Quantum Dot Single-Photon Turnstile Device,” *Science*, vol. 290, no. 5500, pp. 2282–2285, Dec. 2000.
- [136] C. Santori, D. Fattal, J. Vučković, G. S. Solomon, and Y. Yamamoto, “Indistinguishable photons from a single-photon device,” *Nature*, vol. 419, no. 6907, pp. 594–597, Oct. 2002.
- [137] E. Schöll, L. Hanschke, L. Schweickert, *et al.*, “Resonance Fluorescence of GaAs Quantum Dots with Near-Unity Photon Indistinguishability,” *Nano Letters*, vol. 19, no. 4, pp. 2404–2410, Apr. 2019.
- [138] C. Schimpf, M. Reindl, F. Basso Basset, K. D. Jöns, R. Trotta, and A. Rastelli, “Quantum dots as potential sources of strongly entangled photons: Perspectives and challenges for applications in quantum networks,” *Applied Physics Letters*, vol. 118, no. 10, p. 100 502, Mar. 2021.
- [139] D. Huber, M. Reindl, Y. Huo, *et al.*, “Highly indistinguishable and strongly entangled photons from symmetric GaAs quantum dots,” *Nature Communications*, vol. 8, p. 15 506, May 2017.
- [140] E. Knill, R. Laflamme, and G. J. Milburn, “A scheme for efficient quantum computation with linear optics,” *Nature*, vol. 409, no. 6816, pp. 46–52, Jan. 2001.
- [141] P. Kumar, “Quantum frequency conversion,” *Optics Letters*, vol. 15, no. 24, pp. 1476–1478, Dec. 1990.
- [142] S. Zaske, A. Lenhard, C. A. Keßler, *et al.*, “Visible-to-Telecom Quantum Frequency Conversion of Light from a Single Quantum Emitter,” *Physical Review Letters*, vol. 109, no. 14, p. 147 404, Oct. 2012.
- [143] M. Karpiński, M. Jachura, L. J. Wright, and B. J. Smith, “Bandwidth manipulation of quantum light by an electro-optic time lens,” *Nature Photonics*, vol. 11, no. 1, pp. 53–57, Jan. 2017.

- [144] H.-P. Lo and H. Takesue, “Precise tuning of single-photon frequency using an optical single sideband modulator,” *Optica*, vol. 4, no. 8, pp. 919–923, Aug. 2017.
- [145] A. Fognini, A. Ahmadi, S. J. Daley, M. E. Reimer, and V. Zwiller, “Universal fine-structure eraser for quantum dots,” *Optics Express*, vol. 26, no. 19, pp. 24 487–24 496, Sep. 2018.
- [146] D. L. Moehring, M. J. Madsen, K. C. Younge, *et al.*, “Quantum networking with photons and trapped atoms (Invited),” *JOSA B*, vol. 24, no. 2, pp. 300–315, Feb. 2007.
- [147] L. Fan, C.-L. Zou, M. Poot, *et al.*, “Integrated optomechanical single-photon frequency shifter,” *Nature Photonics*, vol. 10, no. 12, pp. 766–770, Dec. 2016.
- [148] D. M. S. Johnson, J. M. Hogan, S.-w. Chiow, and M. A. Kasevich, “Broadband optical serrodyne frequency shifting,” *Optics Letters*, vol. 35, no. 5, pp. 745–747, Mar. 2010.
- [149] A. Guardiani, “Quantum Engineering at the Single Photon Level,” Ph.D. dissertation, Università degli Studi di Milano-Bicocca, Milano, Apr. 2021.
- [150] J. M. Lukens and P. Lougovski, “Frequency-encoded photonic qubits for scalable quantum information processing,” *Optica*, vol. 4, no. 1, pp. 8–16, Jan. 2017.
- [151] U. Paudel, A. P. Burgers, D. G. Steel, M. K. Yakes, A. S. Bracker, and D. Gammon, “Generation of frequency sidebands on single photons with indistinguishability from quantum dots,” *Physical Review A*, vol. 98, no. 1, p. 011 802, Jul. 2018.
- [152] R. M. Stevenson, R. J. Young, P. Atkinson, K. Cooper, D. A. Ritchie, and A. J. Shields, “A semiconductor source of triggered entangled photon pairs,” *Nature*, vol. 439, no. 7073, pp. 179–182, Jan. 2006.
- [153] D. Huber, M. Reindl, S. F. Covre da Silva, *et al.*, “Strain-Tunable GaAs Quantum Dot: A Nearly Dephasing-Free Source of Entangled Photon Pairs on Demand,” *Physical Review Letters*, vol. 121, no. 3, p. 033 902, Jul. 2018.
- [154] T. Lettner, S. Gyger, K. D. Zeuner, *et al.*, “Strain-Controlled Quantum Dot Fine Structure for Entangled Photon Generation at 1550 nm,” *Nano Letters*, Dec. 2021.
- [155] K. D. Zeuner, M. Paul, T. Lettner, *et al.*, “A stable wavelength-tunable triggered source of single photons and cascaded photon pairs at the telecom C-band,” *Applied Physics Letters*, vol. 112, no. 17, p. 173 102, Apr. 2018.
- [156] M. Peres, *The Focal Encyclopedia of Photography*, Fourth. 2013.
- [157] A. Migdall, S. Polyakov, J. Fan, and J. Bienfang, Eds., *Single-Photon Generation and Detection: Experimental Methods in the Physical Sciences* (Experimental Methods in the Physical Sciences). Amsterdam ; Boston: Elsevier/AP, Academic Press is an imprint of Elsevier, 2013, vol. 45.

- [158] D. Salvoni, M. Ejrnaes, L. Parlato, *et al.*, “Lidar techniques for a SNSPD-based measurement,” *Journal of Physics: Conference Series*, vol. 1182, p. 012014, Feb. 2019.
- [159] C. Schuck, W. H. P. Pernice, X. Ma, and H. X. Tang, “Optical time domain reflectometry with low noise waveguide-coupled superconducting nanowire single-photon detectors,” *Applied Physics Letters*, vol. 102, no. 19, p. 191104, May 2013.
- [160] A. Korneev, A. Lipatov, O. Okunev, *et al.*, “GHz counting rate NbN single-photon detector for IR diagnostics of VLSI CMOS circuits,” *Microelectronic Engineering*, Proceedings of the Symposium and Summer School on: Nano and Giga Challenges in Microelectronics Research and Opportunities in Russia, vol. 69, no. 2, pp. 274–278, Sep. 2003.
- [161] M. J. R. Previte, C. Zhou, M. Kellinger, *et al.*, “DNA sequencing using polymerase substrate-binding kinetics,” *Nature Communications*, vol. 6, no. 1, p. 5936, Jan. 2015.
- [162] X. Michalet, O. H. W. Siegmund, J. V. Vallerga, P. Jelinsky, J. E. Millaud, and S. Weiss, “Detectors for single-molecule fluorescence imaging and spectroscopy,” *Journal of Modern Optics*, vol. 54, no. 2-3, pp. 239–281, Jan. 2007.
- [163] R. Rigler and E. S. Elson, *Fluorescence Correlation Spectroscopy Theory and Applications*. Berlin: Springer Berlin, 2013.
- [164] J. Chang, J. W. N. Los, J. O. Tenorio-Pearl, *et al.*, “Detecting telecom single photons with 99.5-2.07+0.5% system detection efficiency and high time resolution,” *APL Photonics*, vol. 6, no. 3, p. 036114, Mar. 2021.
- [165] B. Korzh, Q.-Y. Zhao, J. P. Allmaras, *et al.*, “Demonstration of sub-3 ps temporal resolution with a superconducting nanowire single-photon detector,” *Nature Photonics*, vol. 14, no. 4, pp. 250–255, Apr. 2020.
- [166] D. V. Reddy, R. R. Nerem, S. W. Nam, R. P. Mirin, and V. B. Verma, “Superconducting nanowire single-photon detectors with 98% system detection efficiency at 1550 nm,” *Optica*, vol. 7, no. 12, pp. 1649–1653, Dec. 2020.
- [167] G. N. Gol’tsman, O. Okunev, G. Chulkova, *et al.*, “Picosecond superconducting single-photon optical detector,” *Applied Physics Letters*, vol. 79, no. 6, pp. 705–707, Aug. 2001.
- [168] A. D. Semenov, G. N. Gol’tsman, and A. A. Korneev, “Quantum detection by current carrying superconducting film,” *Physica C: Superconductivity*, vol. 351, no. 4, pp. 349–356, Apr. 2001.
- [169] W. Słysz, M. Węgrzecki, J. Bar, *et al.*, “Fiber-coupled single-photon detectors based on NbN superconducting nanostructures for practical quantum cryptography and photon-correlation studies,” *Applied Physics Letters*, vol. 88, no. 26, p. 261113, Jun. 2006.
- [170] W. H. P. Pernice, C. Schuck, O. Minaeva, *et al.*, “High-speed and high-efficiency travelling wave single-photon detectors embedded in nanophotonic circuits,” *Nature Communications*, vol. 3, ncomms2307, Dec. 2012.

- [171] J. P. Sprengers, A. Gaggero, D. Sahin, *et al.*, “Waveguide superconducting single-photon detectors for integrated quantum photonic circuits,” *Applied Physics Letters*, vol. 99, no. 18, p. 181110, Oct. 2011.
- [172] S. Miki, T. Yamashita, M. Fujiwara, M. Sasaki, and Z. Wang, “Multichannel SNSPD system with high detection efficiency at telecommunication wavelength,” *Optics Letters*, vol. 35, no. 13, pp. 2133–2135, Jul. 2010.
- [173] F. Marsili, V. B. Verma, J. A. Stern, *et al.*, “Detecting single infrared photons with 93% system efficiency,” *Nature Photonics*, vol. 7, no. 3, pp. 210–214, Mar. 2013.
- [174] B. Baek, A. E. Lita, V. Verma, and S. W. Nam, “Superconducting a-WxSi1-x nanowire single-photon detector with saturated internal quantum efficiency from visible to 1850 nm,” *Applied Physics Letters*, vol. 98, no. 25, p. 251105, Jun. 2011.
- [175] Y. P. Korneeva, D. Y. Vodolazov, A. V. Semenov, *et al.*, “Optical Single-Photon Detection in Micrometer-Scale NbN Bridges,” *Physical Review Applied*, vol. 9, no. 6, p. 064037, Jun. 2018.
- [176] C. Becher, W. Gao, S. Kar, *et al.*, “2022 Roadmap for Materials for Quantum Technologies,” *arXiv:2202.07309 [quant-ph]*, Feb. 2022.
- [177] I. Esmail Zadeh, J. Chang, J. W. N. Los, *et al.*, “Superconducting nanowire single-photon detectors: A perspective on evolution, state-of-the-art, future developments, and applications,” *Applied Physics Letters*, vol. 118, no. 19, p. 190502, May 2021.
- [178] A. Engel, J. J. Renema, K. Il’in, and A. Semenov, “Detection mechanism of superconducting nanowire single-photon detectors,” *Superconductor Science and Technology*, vol. 28, no. 11, p. 114003, Sep. 2015.
- [179] D. Y. Vodolazov, “Minimal Timing Jitter in Superconducting Nanowire Single-Photon Detectors,” p. 8, 2019.
- [180] J. Allmaras, A. Kozorezov, B. Korzh, K. Berggren, and M. Shaw, “Intrinsic Timing Jitter and Latency in Superconducting Nanowire Single-photon Detectors,” *Physical Review Applied*, vol. 11, no. 3, p. 034062, Mar. 2019.
- [181] J. P. Allmaras, “Modeling and Development of Superconducting Nanowire Single-Photon Detectors,” Ph.D. dissertation, California Institute of Technology, Jun. 2020.
- [182] V. B. Verma, B. Korzh, A. B. Walter, *et al.*, “Single-photon detection in the mid-infrared up to 10 μ m wavelength using tungsten silicide superconducting nanowire detectors,” *APL Photonics*, vol. 6, no. 5, p. 056101, May 2021.
- [183] J. Chang, J. W. N. Los, R. Gourgues, *et al.*, “Efficient mid-infrared single-photon detection using superconducting NbTiN nanowires with high time resolution in a Gifford-McMahon cryocooler,” *Photonics Research*, vol. 10, no. 4, pp. 1063–1070, Apr. 2022.
- [184] Z. Lin, L. Schweickert, S. Gyger, K. D. Jöns, and V. Zwiller, “Efficient and versatile toolbox for analysis of time-tagged measurements,” *Journal of Instrumentation*, vol. 16, no. 08, T08016, Aug. 2021.

- [185] I. Esmail Zadeh, J. W. N. Los, R. B. M. Gourgues, *et al.*, “Efficient Single-Photon Detection with 7.7 ps Time Resolution for Photon-Correlation Measurements,” *ACS Photonics*, vol. 7, no. 7, pp. 1780–1787, Jul. 2020.
- [186] D. Zhu, M. Colangelo, B. A. Korzh, *et al.*, “Superconducting nanowire single-photon detector with integrated impedance-matching taper,” *Applied Physics Letters*, vol. 114, no. 4, p. 042 601, Jan. 2019.
- [187] R. W. Klopfenstein, “A Transmission Line Taper of Improved Design,” *Proceedings of the IRE*, vol. 44, no. 1, pp. 31–35, Jan. 1956.
- [188] R. Gourgues, J. W. N. Los, J. Zichi, *et al.*, “High performance superconducting nanowire single photon detectors operating at temperature from 4 to 7 K,” *arXiv:1906.09969 [physics]*, Jun. 2019.
- [189] T. Polakovic, W. R. Armstrong, V. Yefremenko, *et al.*, “Superconducting nanowires as high-rate photon detectors in strong magnetic fields,” *Nuclear Instruments and Methods in Physics Research Section A: Accelerators, Spectrometers, Detectors and Associated Equipment*, vol. 959, p. 163 543, Apr. 2020.
- [190] T. Polakovic, W. Armstrong, G. Karapetrov, Z.-E. Meziani, and V. Novosad, “Unconventional Applications of Superconducting Nanowire Single Photon Detectors,” *Nanomaterials*, vol. 10, no. 6, p. 1198, Jun. 2020.
- [191] E. E. Wollman, V. B. Verma, A. B. Walter, *et al.*, “Recent advances in superconducting nanowire single-photon detector technology for exoplanet transit spectroscopy in the mid-infrared,” *Journal of Astronomical Telescopes, Instruments, and Systems*, vol. 7, no. 1, p. 011 004, Jan. 2021.
- [192] I. E. Zadeh, J. W. N. Los, R. B. M. Gourgues, *et al.*, “Efficient Single-Photon Detection with 7.7 ps Time Resolution for Photon-Correlation Measurements,” *ACS Photonics*, vol. 7, no. 7, pp. 1780–1787, Jul. 2020.
- [193] C. Zhang, W. Zhang, J. Huang, *et al.*, “NbN superconducting nanowire single-photon detector with an active area of 300 Mm-in-diameter,” *AIP Advances*, vol. 9, no. 7, p. 075 214, Jul. 2019.
- [194] I. Charaev, Y. Morimoto, A. Dane, A. Agarwal, M. Colangelo, and K. K. Berggren, “Large-area microwire MoSi single-photon detectors at 1550 nm wavelength,” *Applied Physics Letters*, vol. 116, no. 24, p. 242 603, Jun. 2020.
- [195] Y. Hochberg, I. Charaev, S.-W. Nam, V. Verma, M. Colangelo, and K. K. Berggren, “Detecting Sub-GeV Dark Matter with Superconducting Nanowires,” *Physical Review Letters*, vol. 123, no. 15, p. 151 802, Oct. 2019.
- [196] M. S. Allman, V. B. Verma, M. Stevens, *et al.*, “A near-infrared 64-pixel superconducting nanowire single photon detector array with integrated multiplexed readout,” *Applied Physics Letters*, vol. 106, no. 19, p. 192 601, May 2015.
- [197] E. E. Wollman, V. B. Verma, A. E. Lita, *et al.*, “Kilopixel array of superconducting nanowire single-photon detectors,” *Optics Express*, vol. 27, no. 24, pp. 35 279–35 289, Nov. 2019.

- [198] Q.-Y. Zhao, D. Zhu, N. Calandri, *et al.*, “Single-photon imager based on a superconducting nanowire delay line,” *Nature Photonics*, vol. 11, no. 4, pp. 247–251, Apr. 2017.
- [199] J. Chiles, S. M. Buckley, A. Lita, *et al.*, “Superconducting microwire detectors based on WSi with single-photon sensitivity in the near-infrared,” *Applied Physics Letters*, vol. 116, no. 24, p. 242 602, Jun. 2020.
- [200] S. Doerner, A. Kuzmin, S. Wuensch, *et al.*, “Frequency-multiplexed bias and readout of a 16-pixel superconducting nanowire single-photon detector array,” *Applied Physics Letters*, vol. 111, no. 3, p. 032 603, Jul. 2017.
- [201] S. Miyajima, M. Yabuno, S. Miki, T. Yamashita, and H. Terai, “High-time-resolved 64-channel single-flux quantum-based address encoder integrated with a multi-pixel superconducting nanowire single-photon detector,” *Optics Express*, vol. 26, no. 22, pp. 29 045–29 054, Oct. 2018.
- [202] Q. Chen, B. Zhang, L. Zhang, *et al.*, “Sixteen-Pixel NbN Nanowire Single Photon Detector Coupled With 300- μ m Fiber,” *IEEE Photonics Journal*, vol. 12, no. 1, pp. 1–12, Feb. 2020.
- [203] J. P. Allmaras, E. E. Wollman, A. D. Beyer, *et al.*, “Demonstration of a Thermally Coupled Row-Column SNSPD Imaging Array,” *Nano Letters*, vol. 20, no. 3, pp. 2163–2168, Mar. 2020.
- [204] C. L. Lv, H. Zhou, H. Li, *et al.*, “Large active area superconducting single-nanowire photon detector with a 100 μ m diameter,” *Superconductor Science and Technology*, vol. 30, no. 11, p. 115 018, Oct. 2017.
- [205] S. Steinhauer, S. Gyger, and V. Zwiller, “Progress on large-scale superconducting nanowire single-photon detectors,” *Applied Physics Letters*, vol. 118, no. 10, p. 100 501, Mar. 2021.
- [206] R. Cheng, S. Wang, and H. X. Tang, “Superconducting nanowire single-photon detectors fabricated from atomic-layer-deposited NbN,” *Applied Physics Letters*, vol. 115, no. 24, p. 241 101, Dec. 2019.
- [207] R. Cheng, J. Wright, H. G. Xing, D. Jena, and H. X. Tang, “Epitaxial niobium nitride superconducting nanowire single-photon detectors,” *Applied Physics Letters*, vol. 117, no. 13, p. 132 601, Sep. 2020.
- [208] N. Calandri, Q.-Y. Zhao, D. Zhu, A. Dane, and K. K. Berggren, “Superconducting nanowire detector jitter limited by detector geometry,” *Applied Physics Letters*, vol. 109, no. 15, p. 152 601, Oct. 2016.
- [209] F. Marsili, F. Najafi, E. Dauler, *et al.*, “Single-Photon Detectors Based on Ultranarrow Superconducting Nanowires,” *Nano Letters*, vol. 11, no. 5, pp. 2048–2053, May 2011.
- [210] M. Colangelo, B. Korzh, J. P. Allmaras, *et al.*, “Impedance-matched differential superconducting nanowire detectors,” *arXiv:2108.07962 [physics]*, Aug. 2021.
- [211] M. Hofherr, M. Arndt, K. Il’in, *et al.*, “Time-Tagged Multiplexing of Serially Biased Superconducting Nanowire Single-Photon Detectors,” *IEEE*

- Transactions on Applied Superconductivity*, vol. 23, no. 3, pp. 2 501 205–2 501 205, Jun. 2013.
- [212] A. W. Elshaari, A. Iovan, S. Gyger, *et al.*, “Dispersion engineering of superconducting waveguides for multi-pixel integration of single-photon detectors,” *APL Photonics*, vol. 5, no. 11, p. 111 301, Nov. 2020.
 - [213] M. Yabuno, S. Miyajima, S. Miki, S. Miki, and H. Terai, “Scalable implementation of a superconducting nanowire single-photon detector array with a superconducting digital signal processor,” *Optics Express*, vol. 28, no. 8, pp. 12 047–12 057, Apr. 2020.
 - [214] M. A. Wolff, F. Beutel, J. Schütte, *et al.*, “Broadband waveguide-integrated superconducting single-photon detectors with high system detection efficiency,” *Applied Physics Letters*, vol. 118, no. 15, p. 154 004, Apr. 2021.
 - [215] J. Münzberg, A. Vetter, F. Beutel, *et al.*, “Superconducting nanowire single-photon detector implemented in a 2D photonic crystal cavity,” *Optica*, vol. 5, no. 5, pp. 658–665, May 2018.
 - [216] S. Ferrari, C. Schuck, and W. Pernice, “Waveguide-integrated superconducting nanowire single-photon detectors,” *Nanophotonics*, vol. 7, no. 11, pp. 1725–1758, 2018.
 - [217] A. A. Sayem, R. Cheng, S. Wang, and H. X. Tang, “Lithium-niobate-on-insulator waveguide-integrated superconducting nanowire single-photon detectors,” *Applied Physics Letters*, vol. 116, no. 15, p. 151 102, Apr. 2020.
 - [218] E. Lomonte, M. A. Wolff, F. Beutel, *et al.*, “Single-photon detection and cryogenic reconfigurability in lithium niobate nanophotonic circuits,” *Nature Communications*, vol. 12, no. 1, p. 6847, Nov. 2021.
 - [219] R. Raussendorf and H. J. Briegel, “A One-Way Quantum Computer,” *Physical Review Letters*, vol. 86, no. 22, pp. 5188–5191, May 2001.

Part II

Papers

Summary of the Papers

Paper 1

Reconfigurable Photonics with On-Chip Single-Photon Detectors

Integrated quantum photonics offers a promising path to scale up quantum optics experiments by miniaturizing and stabilizing complex laboratory setups. Central elements of quantum integrated photonics are quantum emitters, memories, detectors, and reconfigurable photonic circuits. In particular, integrated detectors not only offer optical readout but, when interfaced with reconfigurable circuits, allow feedback and adaptive control, crucial for deterministic quantum teleportation, training of neural networks, and stabilization of complex circuits. However, the heat generated by thermally reconfigurable photonics is incompatible with heat-sensitive superconducting single-photon detectors, and thus their on-chip co-integration remains elusive. Here we show low-power microelectromechanical reconfiguration of integrated photonic circuits interfaced with superconducting single-photon detectors on the same chip. We demonstrate three key functionalities for photonic quantum technologies: 28 dB high-extinction routing of classical and quantum light, 90 dB high-dynamic range single-photon detection, and stabilization of optical excitation over 12 dB power variation. Our platform enables heat-load free reconfigurable linear optics and adaptive control, critical for quantum state preparation and quantum logic in large-scale quantum photonics applications.

Paper 2

Rydberg excitons in Cu₂O microcrystals grown on a silicon platform

Cuprous oxide (Cu₂O) is a semiconductor with large exciton binding energy and significant technological importance in applications such as photovoltaics and solar water splitting. It is also a superior material system for quantum optics that enabled the observation of intriguing phenomena, such as Rydberg excitons as solid-state analogue to highly-excited atomic states. Previous experiments related to excitonic properties focused on natural bulk crystals due to major difficulties in growing high-quality synthetic samples. Here, the growth of Cu₂O microcrystals with excellent optical material quality and very low point defect levels is presented. A scalable thermal oxidation process is used that is

ideally suited for integration on silicon, demonstrated by on-chip waveguide-coupled Cu_2O microcrystals. Moreover, Rydberg excitons in site-controlled Cu_2O microstructures are shown, relevant for applications in quantum photonics. This work paves the way for the wide-spread use of Cu_2O in optoelectronics and for the development of novel device technologies.

Paper 3

Enhancing Si_3N_4 Waveguide Nonlinearity with Heterogeneous Integration of Few-Layer WS_2

The heterogeneous integration of low-dimensional materials with photonic waveguides has spurred wide research interest. Here, we report on the experimental investigation and the numerical modeling of enhanced nonlinear pulse broadening in silicon nitride waveguides with the heterogeneous integration of few-layer WS_2 . After transferring a few-layer WS_2 flake of $\approx 14.8\text{ }\mu\text{m}$, the pulse spectral broadening in a dispersion-engineered silicon nitride waveguide has been enhanced by $\approx 48.8\%$ in bandwidth. Through numerical modeling, an effective nonlinear coefficient higher than $600\text{ m}^{-1}\text{ W}^{-1}$ has been retrieved for the heterogeneous waveguide indicating an enhancement factor of larger than 300 with respect to the pristine waveguide at a wavelength of 800 nm. With further advances in two-dimensional material fabrication and integration techniques, on-chip heterostructures will offer another degree of freedom for waveguide engineering, enabling high-performance nonlinear optical devices, such as frequency combs and quantum light sources.

Paper 4

Deterministic Integration of HBN Emitter in Silicon Nitride Photonic Waveguide

Hybrid integration provides an important avenue for incorporating atom-like solid-state single-photon emitters into photonic platforms that possess no optically-active transitions. Hexagonal boron nitride (hBN) is particularly interesting quantum emitter for hybrid integration, as it provides a route for room-temperature quantum photonic technologies, coupled with its robustness and straightforward activation. Despite the recent progress of integrating hBN emitters in photonic waveguides, a deterministic, site-controlled process remains elusive. Here, the integration of selected hBN emitter in silicon nitride waveguide is demonstrated. A small misalignment angle of 4° is shown between the emission-dipole orientation and the waveguide propagation direction. The integrated emitter maintains high single-photon purity despite subsequent encapsulation and nanofabrication steps, delivering quantum light with zero delay second order correlation function $g^{(2)}(0) = 0.1 \pm 0.05$. The results provide an important step toward deterministic, large scale, quantum photonic circuits at room temperature using atom-like single-photon emitters.

Paper 5

Engineering the Luminescence and Generation of Individual Defect Emitters in Atomically Thin MoS₂

We demonstrate the on-demand creation and positioning of photon emitters in atomically thin MoS₂ with very narrow ensemble broadening and negligible background luminescence. Focused helium-ion beam irradiation creates 100s to 1000s of such mono-typical emitters at specific positions in the MoS₂ monolayers. Individually measured photon emitters show antibunching behavior with a $g^{(2)}(0) = 0.23$ and $g^{(2)}(0) = 0.27$. From a statistical analysis, we extract the creation yield of the He-ion induced photon emitters in MoS₂ as a function of the exposed area, as well as the total yield of single emitters as a function of the number of He ions when single spots are irradiated by He ions. We reach probabilities as high as 18% for the generation of individual and spectrally clean photon emitters per irradiated single site. Our results firmly establish 2D materials as a platform for photon emitters with unprecedented control of position as well as photophysical properties owing to the all-interfacial nature.

Paper 6

Reconfigurable frequency coding of triggered single photons in the telecom C-band

In this work, we demonstrate reconfigurable frequency manipulation of quantum states of light in the telecom C-band. Triggered single photons are encoded in a superposition state of three channels using sidebands up to 53 GHz created by an off-the-shelf phase modulator. The single photons are emitted by an InAs/GaAs quantum dot grown by metal-organic vapor-phase epitaxy within the transparency window of the backbone fiber optical network. A cross-correlation measurement of the sidebands demonstrates the preservation of the single photon nature; an important prerequisite for future quantum technology applications using the existing telecommunication fiber network.

Paper 7

Strain-Controlled Quantum Dot Fine Structure for Entangled Photon Generation at 1550 nm

Entangled photon generation at 1550 nm in the telecom C-band is of critical importance as it enables the realization of quantum communication protocols over long distance using deployed telecommunication infrastructure. InAs epitaxial quantum dots have recently enabled on-demand generation of entangled photons in this wavelength range. However, time-dependent state evolution, caused by the fine-structure splitting, currently limits the fidelity to a specific entangled state. Here, we show fine-structure suppression for InAs quantum dots using micromachined piezoelectric actuators and demonstrate generation of highly entangled photons at 1550 nm. At the lowest fine-structure setting, we obtain a maximum fidelity of $(90.0 \pm 2.7)\%$ (concurrence of $(87.5 \pm 3.1)\%$). The concurrence remains high also for moderate (weak) temporal filtering, with

values close to 80 % (50 %), corresponding to 30 % (80 %) of collected photons, respectively. The presented fine-structure control opens the way for exploiting entangled photons from quantum dots in fiber-based quantum communication protocols.

Paper 8

NbTiN Thin Films for Superconducting Photon Detectors on Photonic and Two-Dimensional Materials

Integration of superconducting devices on photonic platforms opens up a wide range of functionalities and applications. We report on NbTiN thin films deposited on SiO₂, Si₃N₄, GaAs, LiNbO₃, and AlN as well as on a monolayer of hexagonal boron nitride, using a universal reactive co-sputtering recipe. The morphology and the superconducting properties of the NbTiN thin films with a thickness of 10 nm were characterized by atomic force microscopy and electrical transport measurements. Superconducting strip photon detectors were fabricated using a design suitable for waveguide integration and compared in terms of their internal quantum efficiency and detection pulse kinetics. Our results show well-comparable performances for detectors integrated on different platforms, while also demonstrating that reactive co-sputter deposition of NbTiN at room temperature provides a robust method for realizing superconducting devices on various materials.

Paper 9

Progress on large-scale superconducting nanowire single-photon detectors

Superconducting nanowires have emerged as a powerful tool for detecting single photons in the visible and near-infrared range with excellent device performance metrics. We outline challenges and future directions related to the up-scaling of nanowire devices and detector systems toward widespread applications in demanding real-world settings. Progress on achieving superconducting single-photon detectors with a large active area and an increasing number of pixels is reviewed, comparing the recent literature in terms of the reported key detector parameters. Furthermore, we summarize currently available readout and multiplexing schemes for multi-pixel detector arrays and discuss implications of the recently discovered microwire-based detector geometries.